Comparison and Simulation of a Water Distribution Network in EPANET and a New Generic Graph Trace Analysis Based Model

James Richard Newbold

Thesis submitted to the faculty of the Virginia Polytechnic Institute and State University in partial fulfillment of the requirements for the degree of

Master of Science
In
Environmental Engineering

Dr. Daniel Gallagher
Dr. Andrea Dietrich
Dr. Mark Widdowson

January 27, 2009

Blacksburg, VA

Comparison and Simulation of a Water Distribution Network in EPANET and a New Generic Graph Trace Analysis Based Model

James Richard Newbold

ABSTRACT

The main purpose of this study was to compare the Distributed Engineering Workstation (DEW) and EPANET models. These two models are fundamentally different in the approaches taken to simulate hydraulic systems. To better understand the calculations behind each models' hydraulic simulation, three solution methods were evaluated and compared. The three solution approaches were the Todini, Hardy-Cross, and DEW bisection methods. The Todini method was included in the study because of its similarities to EPANET's hydraulic solution method and the Hardy-Cross solution was included due to its similarities with the DEW approach. Each solution method was used to solve a simple looped network, and the hydraulic solutions were compared. It was determined that all three solution methods predicted flow values that were very similar.

A different, more complex looped network from the solution method comparison was simulated using both EPANET and DEW. Since EPANET is a well established water distribution system model, it was considered the standard for the comparison with DEW. The predicted values from the simulation in EPANET and DEW were compared. This comparison offered insight into the functionality of DEW's hydraulic simulation component. The comparison determined that the DEW model is sensitive to the tolerance value chosen for a simulation. The flow predictions between the DEW and EPANET models became much closer when the tolerance value in DEW was decreased.

Table of Contents

List of Multimedia Objects

Chapter 1 Figures:

Chapter 2 Figures:

Appendix Figures:

Chapter 1: Literature Review

The development and use of predictive models for water distribution systems has been a common practice for many years. In the last twenty years these models have been extended to analyze water quality. These new capabilities are driven by the timely challenge to comply with stringent governmental regulations and customer expectations. With the advancement in computing, water network simulation provides a fast and efficient way of predicting a water network's hydraulic and water quality characteristics. Many modeling programs are now available for commercial and educational use.

1.1 Hydraulics

The use of models has become increasingly important due to the complexity of the topology, size, and constant change of water distribution systems. All of the necessary components must be accounted for in order to develop a representative model of a water distribution system. The following figure illustrates the components, sub-components, and sub-sub-components that comprise a typical water distribution system:

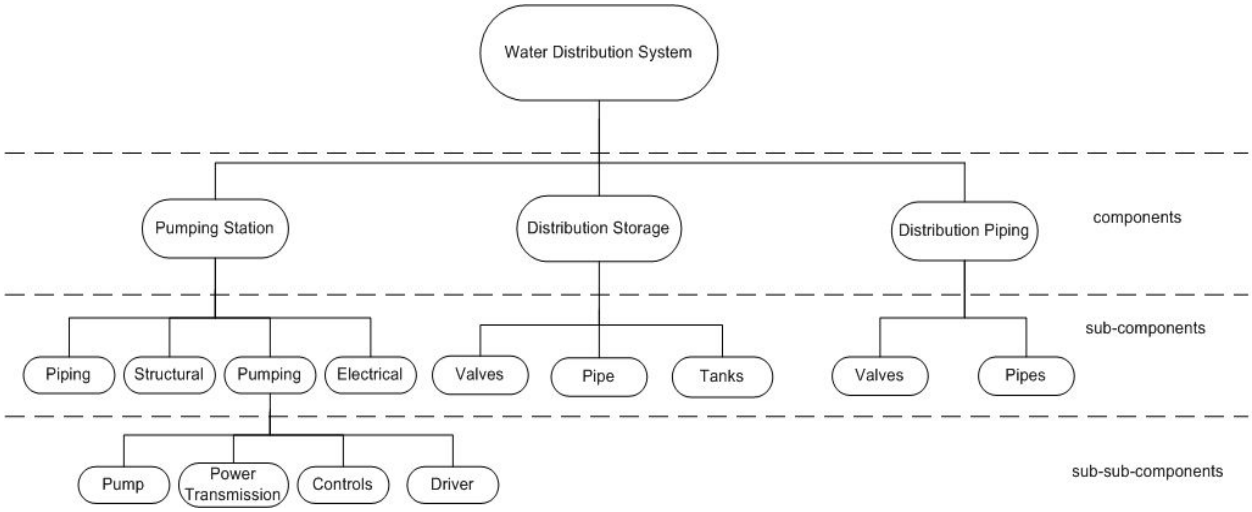

Figure 1.1: Components Comprising a Water Distribution System
(Adapted from Mays, L.W. 2004)

The proper entry of the components' sub-components and sub-sub-components allows a model to simulate the functioning of a water distribution system. Most software such as EPANET, a widely used water distribution network simulator developed by the Environmental Protection Agency (EPA), requires that sub-components for distribution storage and piping be inputted with the necessary information. Pipes, represented as links in EPANET, require the size, length, and roughness (i.e. Hazen-Williams C-factor) of a pipe be entered. Additionally, valves must have the correct size and operating conditions inputted. Further, tanks in EPANET need to be entered with the correct dimensions (i.e. diameter) and operating conditions such as minimum water level, maximum water level, and starting water level. These conditions allow tanks to function as floating tanks, because during the course of a simulation, a tank may fill up or supply the distribution system depending upon current demands. As illustrated in Figure 1.1, pumping stations are rather complicated containing both sub-components and sub-sub-components. In EPANET, pumps are simulated mainly using a pump curve that relates the pressure head to flow. These curves allow pumps to function within the manufacturer's specifications. Pumps are also controlled by other operating conditions such as tank levels and nodal pressures through the use of controls and time patterns. To determine the operating point on a pump curve, a relationship between the system and pump curves must be made. The system head curve is a function of the pipe network in which the pump is located and represents the resistance that the pump must overcome. The following equation is used to determine the system head curve (Rossman, L.A. 2000):

$$h_{system} = h_{stat} + h_f + h_{ML} = \Delta z + h_{req} + h_f + h_{ML} \qquad \text{Eq. 1.1}$$

Where:

h_{stat} = Static head (L)

h_f = Friction head loss (L)

h_{ML} = Minor head loss (L)

Δz = Change in elevation (L)

h_{req} = Required head (L)

The relationship that results between the system head curve and pump curve (Figure 1.2 below) provides insight into the operation of the pump. As seen in Figure 1.2, the intersection of the two curves is the point at which the pump operates.

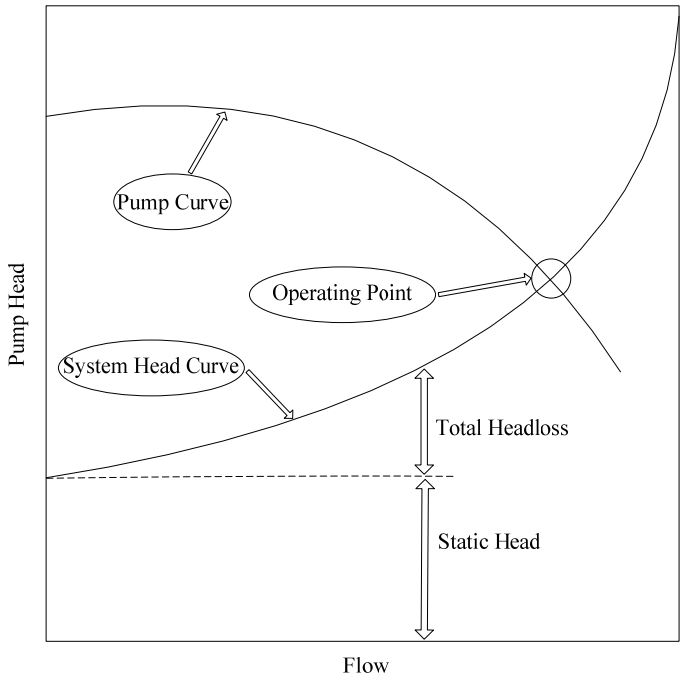

Figure 1.2: Relationship between Pump and System Curve
(*Adapted from Boulus, P. F. 2006*)

Other important uses of a water distribution system model include master planning, rehabilitation, system operation and trouble-shooting. Master planning is the process of projecting system growth and water usage in the future. This allows planners to understand how a system will behave and what improvements are needed to accommodate system growth and

changes in water use. Potentially problematic areas experiencing conditions such as low pressure and low velocity can be identified by a model. With these areas identified, a model can be used to size and locate the addition of new water lines, storage facilities, and pumps to ensure that issues in the problematic areas do not occur.

Rehabilitation of water distribution systems is a major concern for utilities. The infrastructure of distribution systems is aging and the replacement or repair of pipes, valves, tanks, and pumps will be common place. One of the biggest concerns is the aging of unlined, metallic pipes resulting in a buildup of deposits from minerals and chemical reactions in the water. These pipes pose a hydraulic and water quality risk by increasing head-loss and disinfectant depletion. Utilities either scrub and reline the problematic pipes or replace them. Either way, a model can be used to simulate how the distribution system will behave once repairs have been made.

The daily operation of a water distribution system can be simulated using a model to aid an operator in making decisions. If an operator wishes to close a valve or turn off a pump, a model can simulate the changes in the system due to adjusting the current status of a valve or pump. Furthermore, if a utility encounters areas in a system that are experiencing low pressure, a model can be used to troubleshoot the system and identify possible causes such as a partially closed valve. Over the years the use of models has become a cornerstone in water distribution system operation and planning.

1.1.1 Head-Loss Equations

There are a number of head-loss equations that have been developed to determine the frictional losses through a pipe. The three most common equations are the Manning, Hazen-Williams, and Darcy-Weisbach equations. The Manning equation is more typically used for

open channel flow and is dependent on the pipe length and diameter, flow, and the roughness coefficient (Manning roughness). The following is the Manning equation (Walski, T. M. 2003):

$$h_L = \frac{C_f L(nQ)^2}{D^{5.33}} \qquad \text{Eq. 1.2}$$

Where: n = Manning roughness coefficient

C_f = Unit conversion factor (English = 4.66, SI = 10.29)

L = Pipe length (L)

D = Pipe diameter (L)

Q = Pipe Flow (L^3/T)

The Hazen-Williams equation has been used mostly in North America and is distinctive in the use of a C-factor. The C-factor is used to describe the carrying capacity of a pipe. High C-factors represent smooth pipes and low C-factors represent rougher pipes. The following is the Hazen-Williams equation (Walski, T. M. 2003):

$$h_L = \frac{C_f L}{C^{1.852} D^{4.87}} Q^{1.852} \qquad \text{Eq. 1.3}$$

Where:

C = Hazen-Williams C-factor

The Darcy-Weisbach equation was developed using dimensional analysis. This expression uses many of the same variables as the Hazen-Williams equation, but rather than using a C-factor it uses a friction factor, f. The following is the Darcy-Weisbach equation (Walski, T. M. 2003):

$$h_L = \frac{8fLQ^2}{gD^5\pi^2} \qquad \text{Eq. 1.4}$$

Where:

f = Darcy-Weisbach friction factor

g = Gravitational acceleration constant (L/T^2)

Several different methods have been developed for estimating the friction factor, f. Two of the main methods are the Colebrook-White and Swamee-Jain equations. The Colebrook-White equation is one of the earliest approximation methods that relate the friction factor to the Reynolds number and relative roughness. The following is the Colebrook-White equation (Walski, T. M. 2003):

$$\frac{1}{\sqrt{f}} = -0.86\ln\left(\frac{\varepsilon}{3.7D} + \frac{2.51}{Re\sqrt{f}}\right) \qquad \text{Eq. 1.5}$$

Where:

ε = Equivalent roughness

Re = Reynolds number

The main issue with this equation is that the friction factor is found on both sides of the expression. This requires one to solve the expression iteratively to determine which value of the friction factor satisfies the equation. This resulted in the development of the Moody diagram which is a graphical solution for the friction factor. The Swamee-Jain equation is considered to be much easier to solve than the iterative Colebrook-White equation. The following is the Swamee-Jain expression (Walski, T. M. 2003):

$$f = \frac{1.325}{\left[ln\left(\frac{\varepsilon}{3.7D} + \frac{5.74}{Re^{0.9}}\right)\right]^2} \qquad \text{Eq. 1.6}$$

The relative simplicity and accuracy of the Swamee-Jain equation has influenced water distribution system model developers to use this equation to solve for the friction factor.

To better understand certain advantages and disadvantages between the Darcy-Weisbach and Hazen-Williams solutions a study by Usman et al. (1988) was conducted that compared the results of a flow model using these two head-loss equations. This study compared the

Colebrook-White and Hazen-Williams flow models in a real-time water network simulation. The Colebrook-White equation was the method used to determine the friction factor for the Darcy-Weisbach equation. The Hazen-Williams method is more advantageous to the Colebrook-White method due to its simplicity. However, problems arise due to the approximate solution formed by the Hazen-Williams equation, mainly because of the wide range of flows that exist in a real-time water distribution network. The Colebrook-White equation has been widely accepted as more suitable for determining an accurate solution when a wide flow range is present (Usman et al. 1988). This paper discussed an example that was used to evaluate both approaches. The research showed that as the network increased in size (i.e. more nodes) the Colebrook-White equation took longer to converge because the resistance needed to be recalculated every time the flow changed. The Hazen-Williams approach had a time saving advantage over the Colebrook-White method in that the pipe resistance (C-factor) is not a function of flow. Since the Hazen-Williams equation does not account for water temperature, it is not very suitable for varying water conditions. The Colebrook-White equation on the other hand is explicitly dependent on the kinematic viscosity of water which is a function of temperature. This attribute makes the Colebrook equation suitable for a water network simulation that has varying water conditions. Usman et al. (1988) claimed that after comparing the two approaches the Colebrook-White equation was more suitable for real-time simulation where there is a range of flow conditions.

1.1.2 Network Solution Techniques

Network solution methods have evolved from applications where networks were solved by hand calculations to solutions supported by computer hardware. One of the earliest and most well known solution methods is the Hardy-Cross method. This method was developed by a structural engineer to solve head-loss equations in a looped network, and is traditionally solved

iteratively by hand calculations. Within a network with multiple loops, the Hardy-Cross method determines a loop equation for each loop and solves one loop at a time. This method requires a flow balance before the first iteration (the initial guessed flow directions do not need to be correct). The following is the loop equation for a closed loop (Walski, T. M. 2003):

$$Loop\ Equation = \sum_{l=1}^{N} K_l |Q_l|^n\ Sign(Q) \qquad \text{Eq. 1.7}$$

Where:

$K_l = K_u \frac{L}{D^{4.87} C_{HW}^n}$ (for Hazen-Williams)

Q_l = Flow through pipe "l" (L^3/T)

N = Number of loops

n = Value based on which head-loss equation used (i.e. 1.852 for Hazen-Williams)

Equation 1.7 is essentially the sum of the head-loss in a predefined direction around a closed loop. Once the loop equation has been determined, the change in flow for that iteration must be calculated. The equation for the change in flow for a closed loop is (Walski, T. M. 2003):

$$\Delta Q_{LP} = -\frac{\sum_{l=1}^{N} K_l |Q_l|^n Sign(Q)}{\sum_{l=1}^{N} n |h_{L,l}/Q_l|} \qquad \text{Eq. 1.8}$$

Where:

$\sum_{l \in lloop} K_l |Q_l|^n Sign(Q)$ = Loop equation (sum of head-loss around a loop)

N = Number of loops

n = Value based on which head-loss equation used (i.e. 1.852 for Hazen-Williams)

$h_{L,l}$ = Head-loss across pipe "l" (L)

Q_l = Flow through pipe "l" (L^3/T)

At the end of an iteration the change in flow calculated using equation 1.8 is applied to all of the pipes within a respective closed loop. This process is repeated for all of the loops and continues until the change in flow (ΔQ_{LP}) becomes less than some tolerance value.

Once the availability of computer hardware became common place, algorithms that solve the entire network were developed. One of the most commonly used algorithms was developed by Todini et al. (1987) and is called the gradient method. This method allows a modeler to analyze large networks by solving a system of partly linear and non-linear equations that express the balance of mass and energy. This system of equations is comprised of *npipe* and *nnode* equations. The following is the equation used to solve the gradient method (Todini et al. 1987*)*:

$$\begin{matrix} & \textit{npipe} & \textit{nnode} \\ \textit{npipe} \\ \textit{nnode} \end{matrix} \begin{bmatrix} nA_{11} & A_{12} \\ A_{21} & 0 \end{bmatrix} \begin{bmatrix} dQ \\ -- \\ dH \end{bmatrix} = \begin{bmatrix} -dE \\ -- \\ -dq \end{bmatrix} \qquad \text{Eq. 1.9}$$

Where:

n = Value based on which head-loss equation used (i.e. 1.852 for Hazen-Williams)

nA_{11} = Matrix comprised of the derivatives with respect to pipe flow = $nK|Q|^{n-1}$

A_{21} = Connectivity (topological) matrix

A_{12} = Transpose of matrix A_{21}

dQ = Change in pipe flow (L^3/T)

dH = Change in nodal head (L)

-dE = Pipe balance error (L)

-dq = Nodal balance error (L^3/T)

Please note that in equation 1.9 above, the "*npipe*" and "*nnode*" labels signify how the sizes of the matrices depend on the number of pipes and nodes in a system (i.e. nA_{11} is a square npipe x npipe matrix). The result of the nA_{11}, A_{21}, A_{12}, and 0 matrices combined is essentially a

Jacobian matrix for the system. An initial guess for the pipe flows and nodal heads are required for this method, but unlike the Hardy-Cross solution, a flow balance is not required. An advantage of this approach is that all pipe flows and nodal heads are solved in each iteration. This allows the gradient method to converge on a solution in fewer iterations than a method such as Hardy-Cross. This solution method is used by EPANET and allows it to effectively simulate hydraulic parameters in a water distribution network.

The method for solving flow continuity and headloss equations in EPANET is known as a hybrid node-loop approach. This approach is very similar to the solution method designed by Todini et al. (1987) (the gradient method) and was chosen over similar methods due to its simplicity. EPANET begins analysis by selecting initial flow estimates for every pipe in the system. These initial flow estimates are based on a velocity of 1 ft/s through the pipes and are not intended to satisfy continuity. For every iteration of this method, nodal heads are determined by solving the matrix equation AH=F. The term A in the matrix equation is an (NxN) Jacobian matrix, H is an (Nx1) vector of unknown nodal heads, and F is an (Nx1) vector of right hand side terms (Rossman et al. 2000). After new heads are determined using the aforementioned matrix equation, the new flows through the pipes are determined. The advantage of this method is that it solves for the hydraulic parameters at every node within a system simultaneously. This greatly improves the probability of convergence. The criterion for convergence is user defined and is inputted in terms of a tolerance value. For example, if the sum of the absolute flow changes relative to the total flow through all of the pipes in the system is less than some prescribed tolerance (e.g. 0.003), then the process of solving the matrix equation and determining the new flows is terminated.

To better understand how the gradient method developed by Todini et al. (1987) compares to other solution algorithms, Salgado et al. (1988) conducted a study that compared the gradient method to the simultaneous path and linear theory methods. The simultaneous path method is designed to solve all of the loops within a system simultaneously. The following is the expression for the simultaneous path method (Salgado et al. 1988):

$$(\sum_k J_i)\Delta Q_k + \sum_k (J_i \Delta Q_n) = \delta E_k - \sum_k H_i \qquad \text{Eq. 1.10}$$

Where:

J_i = Gradient of head loss in a pipe (H_i/Q_i)

δE_k = Available pressure heads

H_i = Headloss through pipe, "i" (L)

ΔQ_k = Flow correction for all links in a loop, "k" (L^3/T)

The first term on the left side of equation 1.10 accounts for the flow correction that is applied to the pipes in loop "k", while the second term accounts for the effect of the flow correction in the neighboring loops. The right side of equation 1.10 is the difference between the available heads and total head losses in each loop.

The linear theory method requires the simultaneous solution of the following two sets of equations (Salgado et al. 1988):

$$\sum_i Q_{ij} = q_j \quad \text{for all nodes "j"} \qquad \text{Eq. 1.11}$$

Where:

Q_{ij} = Flow through link connecting nodes "i" and "j" (L^3/T)

q_j = Nodal demand in node "j" (L^3/T)

$$\sum_k (J_i Q) = \sum_k (J_i Q_i - H_i) + \delta E_k \quad \text{for all loops "k"} \qquad \text{Eq. 1.12}$$

Equation 1.12 is written for every loop in a network. This version of the linear theory method requires the definition of flow paths, but does not need an initial flow since it generates its own initial flow distribution.

The gradient method proposed by Todini et al. (1987) is defined by equation 1.9. The upper part of equation 1.9 represents the headloss-flow relationship and the lower part corresponds to the nodal flow balance. The simultaneous path and linear theory methods require that a branched network be transformed into an equivalent looped network. To evaluate the three algorithms they were translated into FORTRAN and tested using a series of network examples. The results from the network examples indicated that the simultaneous path and linear theory methods, along with the gradient method, were able to converge on a solution. However the gradient method had certain advantages over the other two solution methods. The main concern with the simultaneous path and linear theory methods was that they were unable to determine the nodal heads when the network contained pipes with small diameters or nearly closed valves. The gradient method was able to converge for every network example with considerable speed. In addition, this method did not have difficulty converging when there were partially closed valves and high resistance pipes present, because it determines both nodal heads and pipe flows at each stage. The gradient method was also able to simulate partially looped and branched systems, whereas the simultaneous path and linear theory methods require an equivalent looped system. Unlike the two other solution methods, the gradient method was able to continue a simulation if a network becomes disjointed (i.e. through the action of valves). Salgado et al. (1988) concluded that the gradient method is more desirable than the simultaneous path and linear theory algorithms due to its ability to converge during extreme cases.

1.1.3 Graph Trace Analysis

Graph trace analysis (GTA) has been in development for nearly twenty years and constitutes a new method in integrated system analysis. Over the past twenty years, GTA has been used to model integrated power transmission and distribution down to the individual consumers for systems composed of millions of components. GTA has also been used to develop real-time monitoring systems for power, water, gas, and sewage. In theory, GTA could be used with any system that can be represented as a well-defined network of interrelated components with definable "through" and "across" characteristics. A "through" characteristic depicts the calculation of variables that flow through components (i.e. flow), and an "across" characteristic depicts the calculation of the variable that is applied across components (i.e. pressure). Advantages of GTA include: allowing a modeler to structure and manage common models, along with performing analyses across multiple system types; developing a model that simulates steady-state, discrete event, and transient scenarios; allowing for the recombination or extension of a system as unforeseen issues arise and priorities change (Feinauer et al. 2008).

In order to perform a simulation with a model, GTA utilizes a one-to-one correspondence between the objects in the model and the components in the physical system. The objects in the model are stored together as a system in a "container." This container provides iterators which algorithms use to access data, perform analyses, and control components. Each component uses iterators to define the relationships with other components and the data stored in the container. Figure 1.2 below illustrates how iterators relate algorithms and results to the rest of the model ("container"). Each component is encountered only one time in a single graph trace from a reference source (i.e. tank) through the network. In GTA every component has only one reference source. Algorithms use the GTA traces and sets formed by iterators to perform

analyses. The following figure illustrates the relationship among algorithms, iterators, and a container (Feinauer et al. 2008):

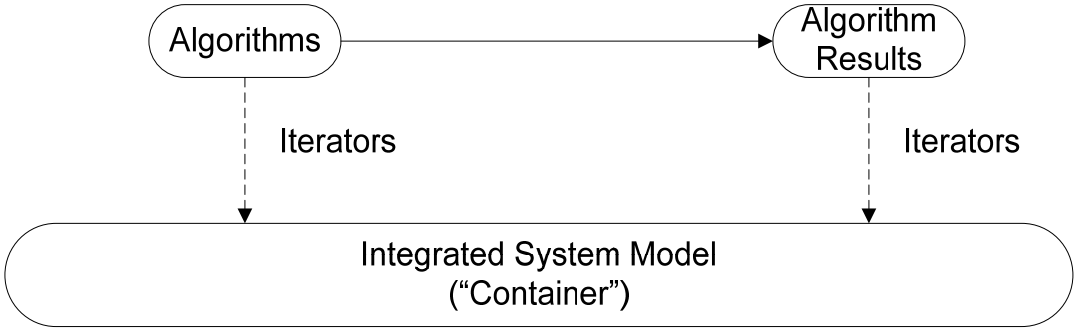

Figure 1.3: Relationship among Algorithms, Iterators, and the Container

GTA uses the concept of graphs to develop sets that are created by tracing through a network. The traces are implemented by iterators (as described above) and set operators. In a GTA model, the components in a system correspond to an edge of a graph. The nodes in a system are not directly modeled but rather become part of the edge itself. This concept means that a GTA model is an edge-edge graph. It is believed that the use of an edge-edge graph rather than a more traditional node-to-node approach is more suitable for integrated, reconfigurable, and very large systems. GTA has the ability to solve edge and loop based iterative analyses that use matrices, loop equation based matrices, and a combination of the two (Feinauer et al. 2008). It is important to note that a GTA model has the ability to store and manage interrelationships within the model itself. This is accomplished by attaching attributes (i.e. algorithm results) to specific components in the model. This capability is also known as in-memory data.

1.1.4 Generic Algorithms (Generic Analysis)

The use of iterators, component objects, system containers and generic algorithms to analyze engineering physical network problems is referred to as "Generic Analysis." Each component in a model is responsible for calculating its internal state and reaction to external influences. Generic algorithms are used to calculate the "through" (i.e. flow) and "across" (i.e. pressure) variables for each component. Due to the nature of distribution systems, numerical iteration is typically required in order for convergence on a solution to occur. In Generic Analysis, all of the components in a system are the container. The trace iterators in GTA are used by generic algorithms to navigate and access contained objects. Generic algorithms are programmed in a model so that calculated results can be related back to the container where they can be accessed by other algorithms. This implies that algorithms can work in unison via the container. For example, if data required by an algorithm has not been calculated, the container can request that an appropriate algorithm perform a calculation to provide the required data. The developers of Generic Analysis refer to this concept as collaborative integration. The use of generic algorithms ultimately allows one to solve a "system of systems" problem that involves interdependencies among different types of systems (i.e. fluid and electrical) (Feinauer et al. 2008).

1.1.5 Hydraulic Calibration

Hydraulic simulation software is developed by collecting and entering the required data. However, a modeler cannot make the assumption that the model is performing accurate simulations. A hydraulic simulation software typically solves the continuity and energy equations using the supplied data. Thus, the quality of the simulations is dependent on the

quality of the data. Therefore, the accuracy of simulation software depends on how well it was calibrated (Walski, T. M. 2003).

Calibration can be defined as the process of comparing a model's results to field observations. If necessary, the input parameters describing a system can be adjusted until the model makes predictions that agree reasonably with measured values. The parameters that may need adjustment may include but are not limited to: system demands, pipe roughness, and pump operating characteristics. The complete calibration of a model allows a modeler to have a better understanding of a distribution system and more confidence in the model's predictions (Walski, T. M. 2003).

Calibrating the hydraulic simulating component of a water distribution system model is an intensive and important step for the proper functioning of the model. Performing a detailed calibration ensures that the model generates results that are accurate and reliable. A number of parameters are necessary for the correct calibration of a model; these include but are not limited to the sizes, locations, and roughness values of the pipes. The sizes and locations of pipes can be determined by measurements in the field and construction drawings, but roughness values are not obtained by direct measurements (Meier et al. 2000). Instead, roughness values need to be determined by back-calculating from the results of flow tests within the system. The best means of conducting a flow test is by opening a hydrant and measuring the flow rate at the open hydrant and the pressure change at the closest upstream hydrant. This method of flow testing is not practical for performing on every hydrant within a large system, thus a select number of representative hydrants are chosen and the roughness values for the system are inferred from those results.

A study by Meier et al. (2000) investigated the use of genetic algorithms in order to determine the best locations to conduct the open hydrant flow tests. Genetic algorithms are a relatively novel concept of optimization that can replace the more common approach in which an experienced modeler determines the best sampling locations on an ad hoc basis. The later method is largely affected by the experience of the modeler. Genetic algorithms are based on the mechanisms of natural selection and genetics. The implementation of a genetic algorithm starts with a random selection of code strings. Each code string is simply a vector containing decision values that points to one location in the solution space (Meier et al. 2000). Once the code strings are populated, the "fittest" strings are selected and passed down to the next generation. In order to improve the probability that favorable traits make it to the next generation, mutation is often used to alter a string to recover or create traits. In this study a sample water distribution network was used as a means to test the optimization capabilities of genetic algorithms. In this case, the genetic algorithm was used to determine the best flow test locations on the standard that the flow tests would produce a non-negligible velocity of 0.30 m/s. The genetic algorithm was validated by determining the optimal locations within the system using complete enumeration (listing all possible solutions) and then comparing the results to those of a genetic algorithm. When compared to the complete enumeration results, the genetic algorithm proved capable of determining the same solution within a reasonable probability. Thus, Meier et al. (2000) concluded that the use of genetic algorithms is a dependable alternative to the more time and memory consuming traditional methods.

Calibration research has developed several different techniques that optimize parameter choices and sampling designs. Studies conducted by Reddy et al. (1996), Bush et al. (1998), Bremond et al. (2003), and Huang et al. (2007) have explored calibration design and

methodology. Reddy et al. (1996) focused on the use of a weighted-regression to identify and remove poor measurements within a data set, which can improve the execution of calibrating a model. The study by Bush et al. (1998) compared three different sensitivity-based methods for optimizing the calibration design. These methods were the Max-Sum design, Max-Min design, and the Weighted-Sum methods. Each of these methods rank spatial measurement locations (i.e. network nodes) or types (i.e. pressure or tracer concentrations) according to a measure of their worth for parameter estimation. The study by Bremond et al. (2003) focused on determining the best locations for calibration measurements. This involved research on the method of minimizing the error in the estimation of chosen parameters to determine the best locations for measurements. Lastly, Huang et al. (2007) researched the use of Bayesian statistical analysis incorporated with Gibbs sampling to estimate specific parameters. These studies offered insight into the extensive research that is being conducted in the area of optimizing the calibration process.

1.1.6 Extended Period Simulation

The transition from steady state to dynamic simulations required the development of a model with the ability to perform extended-period simulations (EPS). In the early stages of EPS development, simulation time periods were too limited, preventing a meaningful long term characterization of a water distribution system. The simulation time for an effective EPS analysis was studied by Harding et al. (2000). At the time of this study the authors claimed that the current EPS simulation times were generally for periods of one or a few days. This study proposed running a hydraulic and water quality simulation for a period of twenty years. This EPS would allow for the reconstruction of the spatial and temporal patterns of contamination in a water distribution system. A modified version of EPANET was used that allowed the time-series

data file to read in such a way so that the results of each daily simulation were used as the initial conditions for the following day. This study concluded that an EPS does not take into account the changes in water use and quality that are inherent in a water distribution system; for instance a period of less water use due to a drought would not be considered. However, an experienced modeler may be able to choose representative time periods to account for these changes, which can reduce inherent deficiencies. The trade-off for using an EPS is that a larger amount of high quality data is needed for longer simulations. If an abundant source of reliable data is available, than an EPS is a viable option for understanding the nature of a water distribution system over a long period of time. The improvement of dynamic simulations in water modeling has allowed for the dynamic modeling of water quality, offering insight into the nature of reactions of chemical constituents.

1.2 Water Quality

Utilities have become increasing concerned with the behavior and transport of chemical species in a water distribution system. Beginning in the mid-eighties, advancements in computer technology allowed for the addition of water quality to hydraulic models. This was motivated by the recognition that water quality can greatly change from the water treatment plant, through the distribution system, and to the consumer. With the advancement in dynamic hydraulic simulations, the long term simulation of water quality within a distribution system became possible.

Most versions of water distribution models contain a water quality modeling package in addition to hydraulic modeling. With the capability of water quality modeling, simulations can be made that improve the understanding of reaction and transport of different chemical constituents. For instance, a tracer study can be conducted which allows a utility to simulate the

transport and reaction of a chemical from when it enters the system from the water treatment plant. A tracer study offers valuable insight into how a system will react to possible contaminants and changes in disinfectant use. A major concern to most utilities is how chlorine residual behaves in a water distribution system. A model can be used to simulate the reaction of chlorine, the formation of disinfectant byproducts, and the impacts on residual concentrations from storage tanks. The information provided by simulating the fate of a disinfectant such as chlorine allows utility operators to plan more effectively.

1.2.1 Simulating Water Quality

The modeling of chlorine decay in a distribution system requires the summed effects of the bulk liquid and pipe wall. Even though zero, first, and second-order decay reactions are used in practice, a first-order reaction is widely accepted when modeling chlorine decay. The following exponential equation is first-order decay (Walski, T. M. 2003):

$$C_t = C_0 e^{-kt} \qquad \text{Eq. 1.13}$$

Where: C = Concentration at time t (M/L^3)

C_0 = Initial Concentration (at time zero) (M/L^3)

k = Reaction rate constant (1/T)

The reaction rate constant (k) in equation 1.13 is the overall reaction rate constant, in that it incorporates both the bulk and wall reaction rate constants. The bulk reaction rate constant will be determined experimentally by obtaining measurements at the distribution network. The wall reaction constant must be evaluated while taking into consideration the mass transfer rate of chlorine between the bulk liquid and pipe wall. The following equation is the relationship among the overall, bulk, and pipe wall reaction rate coefficients (Walski, T. M. 2003):

$$k = k_b + \frac{k_w k_f}{R_H(k_w + k_f)} \qquad \text{Eq. 1.14}$$

Where: k_b = Bulk reaction rate coefficient (1/T)

k_w = Wall reaction rate coefficient (L/T)

k_f = Mass transfer rate coefficient (L/T)

R_H = Hydraulic radius of pipe (L)

The mass transfer rate coefficient (k_f) in equation 1.14 depends on the molecular diffusivity of the constituent in the bulk liquid, the pipe diameter, and the Sherwood number. This relationship is illustrated in the following expression (Walski, T. M. 2003):

$$k_f = \frac{S_H d}{D} \qquad \text{Eq. 1.15}$$

Where: S_H = Sherwood number

d = Molecular diffusivity of constituent in the bulk liquid (L^2/T)

D = Diameter of pipe (L)

The Sherwood number (S_H) in equation 1.15 is a dimensionless parameter that is a function of the Reynolds number (R_e) and kinematic viscosity (ν) of the fluid. The value of the Reynolds number determines the expression used to evaluate the Sherwood number. The following are the expressions that correspond to the appropriate range of Reynolds numbers.

- For stagnant flow (Re < 1) the Sherwood number is equal to 2.0.
- For turbulent flow (Re > 2300) the Sherwood number is evaluated using the following expression (Walski, T. M. 2003):

$$S_H = 0.023 Re^{0.83} \left(\frac{\nu}{d}\right)^{0.333} \qquad \text{Eq. 1.16}$$

Where: Re = Reynolds number

d = Molecular diffusivity (L^2/T)

ν = Kinematic viscosity of liquid (L^2/T)

- For laminar flow (1<Re<2300) the Sherwood number is evaluated using the following expression (Walski, T. M. 2003):

$$S_H = 3.65 + \frac{0.668\left(\frac{D}{L}\right)(Re)\left(\frac{\nu}{d}\right)}{1+0.04\left[\left(\frac{D}{L}\right)Re\left(\frac{\nu}{d}\right)\right]^{2/3}} \quad \text{Eq. 1.17}$$

Where: D = Pipe diameter (L)

L = Length of pipe (L)

Equation 1.17 for the Sherwood number during laminar flow is effectively the average Sherwood number along the entire length of the pipe.

Chlorine decay in water distribution systems is a constant concern to ensure the quality of water received by the consumer. In order to determine the extent to which chlorine residual diminishes, predictive modeling techniques have been developed. A study conducted by Rossman et al. (1994) discusses the development of a mass-transfer-based model for predicting chlorine decay in water distribution networks. This model considers first order reactions of chlorine in both the bulk water and the pipe wall. The following was the equation used to model the reaction rate of chlorine (Rossman et al. 1994):

$$\frac{dc}{dt} = -u\frac{dc}{dx} - Kc \quad \text{Eq. 1.18}$$

$$K = k_b + \frac{k_w k_f}{r_h(k_w k_f)} \quad \text{Eq. 1.19}$$

Where:

u = Flow velocity

K = Overall reaction rate constant (1/T)

c = Chlorine concentration (M/L^3)

k_b = Decay rate constant in bulk flow (1/T)

k_w = Wall reaction rate constant (1/T)

k_f = Mass-transfer coefficient (L/T)

r_h = Hydraulic radius (L)

The rate of the wall reaction is a function of the mass transfer of chlorine to the pipe wall and is thus dependent on pipe geometry and flow. This model was able to illustrate how smaller pipe sizes and higher flow velocities cause an increase in chlorine decay. The model was applied to chlorine measurements taken at nine locations from a portion of the South Central Connecticut Regional Water Authority's (SCCRWA) service area, and used an Eulerian approach called the Discrete Volume Element Method (DVEM) to evaluate the set of differential/algebraic equations for determining the residual chlorine concentrations (Rossman et al. 1994). When hydraulic conditions are constant, DVEM is performed by separating pipes into segments which are treated as completely mixed reactors. Reactions then take place within each segment and the resulting concentrations are transferred to the adjacent downstream segment. Once the reaction and transport steps have completed, the resulting concentration at each junction is determined. This concentration is then released into the end segments of the pipes with the flow leaving the node. This method is repeated until a new hydraulic condition occurs. This DVEM approach can be found in EPANET. The reaction rate constant for bulk flow (k_b) was estimated via lab tests, whereas the pipe wall reaction rate constant (k_w) was adjusted over a range of values (Rossman et al. 1994). The results from this study were compared to observed chlorine measurements. Good agreement between the predicted and observed values was present when hydraulic conditions were well characterized. In cases where hydraulic calibration was not complete, less accurate chlorine predictions resulted. Complete hydraulic calibration was essential for the optimal performance of the model since chlorine kinetics were dependent on flow velocity. This

study emphasizes the importance of hydraulic calibration when determining water quality parameters.

There are two major categories for tracking bulk water in the simulation of water quality in a pipe network: the Eulerian model and the Lagrangian model. For an Eulerian model pipes are divided into equal volume segments and water flows through the volume segments as time progresses and chemical reactions are included in transport. A Lagrangian model tracks parcels of water with homogenous constituent concentrations as they move through a pipe. New parcels can be added due to changes in source quality or when two or more parcels meet at a junction. In order to reduce the number of possible parcels, algorithms have been developed that combine parcels with negligible difference in constituent concentrations. A study by Rossman et al. (1996) compared four different numerical methods, two of which were Eulerian based and two that were Lagrangian based. The two Eulerian based methods are the finite-difference and discrete-volume methods. The two Lagrangian based methods are the time-driven and event-driven methods. This study evaluated the performance of each approach by encoding each method into a water distribution system model and running them on several networks of different size but under identical accuracy tolerances. Five major conclusions were reached after the comparison of accuracy, computation time, and computational storage requirements was completed. The conclusions were as follows:

1. The numerical accuracy of the methods was effectively the same, with the exception that the Eulerian methods had occasional inaccuracies.
2. Each of the methods was capable of representing water quality behavior in existing water distribution systems.
3. Network size was not always an indicator of solution time and memory required.

4. Lagrangian methods were more time and memory efficient than Eulerian methods for modeling chemical constituents.
5. For modeling water age, the Lagrangian time-driven method was the most time efficient whereas the Eulerian methods were the most memory efficient. (Rossman et al. 1996)

Based on the results provided in this study, it seemed that the Lagrangian event-driven method was the most versatile unless there were limitations due to computer memory. If that is the case, the Eulerian methods are preferred.

Chlorine decay in bulk water can be affected by different chemical constituents and conditions. There have been several studies that investigate chlorine decay in different bulk water conditions. Two of these studies, conducted by Boccelli et al.(2003) and Shang et al. (2008), delved into the behavior of reactive chlorine under different conditions and in the presence of different chemical constituents. Boccelli et al. (2003) developed a reactive species model for chlorine decay and trihalomethane (THM) formation under rechlorination conditions. This model involved second-order chlorine decay and total THM formation. The second-order decay model took into account the reactive species involved in the kinetics, which allowed the model to simulate how the chlorine concentration depended upon the reactive species. The following was the second-order equation used in this study (Boccelli et al. 2003):

$$C_A(t) = \frac{C_{A,0} - \alpha}{1 - \left(\frac{\alpha}{C_{A,0}}\right)\exp\left[-\left(\frac{C_{A,0}}{\alpha} - 1\right)\beta t\right]} \qquad \text{Eq. 1.20}$$

$$\propto = \frac{aC_{B,0}}{b} \quad (M/L^3) \qquad \text{Eq. 1.21}$$

$$\beta = k_A C_{B,0} \quad (1/T) \qquad \text{Eq. 1.22}$$

Where:

$C_{A,0}$= Initial concentration of chlorine (M/L^3)

$C_{B,0}$ = Initial concentration of reactive species (M/L^3)

k_A = Second order chlorine decay rate coefficient ($L^3M^{-1}T^{-1}$)

t = Time

(a/b) = Stoichiometric ratio of the chlorine consumed to reactive material consumed

The parameter $\propto$, is the stoichiometric chlorine concentration that is required for the completion of the reaction. This is based on a hypothetical non-reversible reaction that follows $aA + bB => pP$, where A and B are the chlorine component and reactant component respectively and P is the disinfectant by-product. The parameter β in equation 1.22 is a pseudo-first-order decay rate coefficient. In order to determine the chlorine concentration after rechlorination the concentration of the reactant had to be determined since the parameters $\propto$ and β are a function of the reactant concentration. The following equation was used to calculate the reactant concentration after rechlorination (Boccelli et al. 2003):

$$C^*_{B,0} = C_{B,0} - \frac{b}{a}[C_{A,0} - C_A(t_b)] \qquad \text{Eq. 1.23}$$

Where:

$C^*_{B,0}$ = Reactant concentration after rechlorination (M/L^3)

(b/a) = Stoichiometric ratio of the reactive material consumed to the chlorine consumed

$C_A(t_b)$ = Chlorine concentration at time of rechlorination, t_b (M/L^3)

With the new reactant concentration determined using equation 1.23 the parameters $\propto$ and β can be calculated, allowing a new chlorine concentration after rechlorination to be determined using equation 1.20. Boccelli et al. (2003) determined that the second-order model was able to perform as well as or better than the traditional first-order decay model. Additionally, the total THM concentration proved to be linearly related to the amount of chlorine decay and can be defined by the following equation (Boccelli et al. 2003):

$$TTHM(t) = Tx(t) + M \qquad \text{Eq. 1.24}$$

Where:

$x(t) = C_{A,0} - C_A(t_b)$ = Total chlorine demand at time, t

$T = p/a$ = Stoichiometric ratio of TTHM formation and chlorine consumed

M = TTHM concentration at t=0 (M/L^3)

The second-order model developed by Boccelli et al. (2003) has applications in modeling water quality at junctions within a water distribution system. For instance, the water containing a lower chlorine concentration will enter a junction and be rechlorinated by water with a higher chlorine concentration, thus altering the reactive and disinfectant species concentration due to mixing. This application would require the tracing of chlorine and the reactive species within a system.

The development of a model that could simulate the reaction and transport of multiple species in a water distribution system was pursued by Shang et al. (2008). The model developed was able to simulate the reaction of a chemical species with other chemicals, biological material, and organics present in the bulk liquid and pipe wall. This model was created by extending the current version of EPANET to form EPANET-MSX (multispecies extension). Reactions that occur in water within a distribution system are not solely caused by influences in the bulk water, but are also affected by the contact water has with the pipe wall.

1.2.2 Effects of Pipe Wall on Reaction

There has been extensive research on the effects of the pipe wall on chemical reactions. Specifically, researchers have been interested in the effects that a pipe wall has on the depletion of chlorine residual. In order to better understand the effects that different pipe material and age have on chlorine first-order wall decay constants Al Jasser et al. (2006) conducted a study that

involved three hundred and two pipes varying in age, size, and material. The different materials used were: cast iron, steel, asbestos cement, cement-lined cast iron (CLCI), cement-lined ductile iron (CLDI), polyvinyl chloride (PVC), unplasticized polyvinyl chloride (uPVC), and polyethylene. Additionally, the pipe ages ranged from new to fifty years, and the pipe diameters ranged from a half an inch to twelve inches. Water containing a chlorine concentration of 2 mg/l was exposed to the different pipes. Sampling for chlorine residual took place until the concentration was approximately ten percent of the initial concentration. The bulk reaction rate constant, k_b, was determined experimentally using a clean flask and was on average 0.28 day^{-1} with a standard deviation of 0.021 day^{-1}. The wall reaction constant, k_w, observed during the experiment ranged from 0.11 to 112 day^{-1}. This wide range is a result of the varying age, size, and composition of the sample pipes. Al Jasser et al. (2006) made an interesting hypothesis that the layer of biofilm and tubercles can actually prevent some chlorine decay because the reactive surface of the pipe is buffered from the bulk water. In order to test this hypothesis, the biofilm and tubercle layers were removed from several pipes to see if the wall reaction constant would change. This method actually showed that the wall chlorine decay constant increased and decreased depending on the pipe material and age. For medium age steel and cast iron pipes (approximately 18 years old) the removal of the layer caused a decrease in the wall reaction constant of about 7% and 12% respectively. This indicated that the biofilm and tubercle layer was actually a more reactive surface than the bare pipe wall. Conversely, removing the layer from old pipes increased the wall reaction constant by 15% for steel pipes and 18% for cast iron pipes. This indicated that the biofilm and tubercle layer was less of a reactive surface and buffered the more reactive pipe wall from the bulk water. The decrease in the chlorine decay constant for the less aged pipes indicated that the layer was consuming chlorine more than

protecting the pipe wall, whereas the increase in the constant for the more aged pipes showed that the layer was providing protection more than consuming chlorine. These results do provide some insight into the role biofilm and tubercle layers have on chlorine consumption, but further research must be conducted in order to reach a plausible conclusion. The main conclusions drawn from this study are that the pipe service age has a significant impact on the chlorine wall reaction rate and that the wall reaction rate will govern chlorine decay when the bulk reaction rate is less prominent.

1.2.3 Water Quality Calibration

Ensuring that a model is calibrated with respect to water quality simulation is a major concern to any modeler. A thoroughly calibrated water quality model is essential for accurate and confident results. In order to calibrate a water quality model for a reactive constituent, the governing parameters for reaction must be correctly adjusted. However, the calibration of water quality simulation should not occur until the hydraulic simulation component of the model has been completely calibrated. Research has been conducted in water quality calibration and the necessary parameters requiring adjustment. A study conducted by Zheng et al. (2006) explored the process of effectively calibrating a water quality model by adjusting bulk and wall reaction rates. For the bulk reaction rate, the parameters of interest were the bulk reaction coefficient, bulk reaction order, and concentration limit. These parameters needed to be adjusted for both the pipe and tank components in a system. To simplify the calibration process, pipes with similar characteristics (i.e. pipe material and age) were combined into one calibration group for the bulk reaction coefficient adjustment. However, the tank bulk reaction coefficient was calibrated individually for each storage tank. The parameters that needed to be adjusted for pipe wall reaction were the wall reaction coefficient and reaction order. Both of these parameters are

related to pipe material and pipe wall conditions (i.e. tuberculation). This study proposed two different means of calibrating the pipe wall parameters. The first method was known as direct calibration, which is similar to the calibration of the bulk reaction parameters and involved the grouping of pipes with similar characteristics (age, material, and location) and directly optimizing the pipe wall reaction coefficient and reaction order. The second method was known as correlation calibration and involved the assumption that there is a relationship between the increase of pipe wall roughness due to age and the reactivity of the pipe wall. The relationship between the pipe wall reaction coefficient and the pipe roughness varies depending on which head-loss equation is used (Zheng et al. 2006):

Hazen-Williams: $K_w = F/C$ Eq. 1.25

Darcy-Weisbach: $K_w = -F/\log(e/d)$ Eq. 1.26

Chezy-Manning: $K_w = F*N$ Eq. 1.27

Where:

K_w = Pipe wall reaction coefficient

C = Hazen-Williams C-factor

e = Darcy-Weisbach roughness

N = Manning roughness coefficient

d = Pipe diameter (L)

F = Coefficient of correlation

The coefficient of correlation, F, is related to the wall reaction coefficient in a way that is dependent on the head-loss equation used. The parameter F must be determined from site-specific field measurements. The advantage of using correlation calibration is that it requires only a single parameter F, to allow wall reaction coefficients to vary throughout a system in a

physically meaningful way. This is based on the assumption that the hydraulic model is calibrated and that the pipe roughness values are known. The methodology proposed in this study used an example to illustrate the importance of water quality calibration. For this example, the pipe wall reaction rate was calibrated using the correlation method. The results of the study showed that before calibration a large difference existed between the observed and modeled chlorine concentrations, whereas after calibration the model produced chlorine concentrations that were much more representative of the observed values. The necessity of an accurately calibrated hydraulic model was reinforced in this study due to the need of a well calibrated extended period simulation hydraulic model for water quality calibration. If the hydraulic model is not well calibrated, then errors in the hydraulic model can be transferred to the water quality calibration process.

There have been major accomplishments in the development of water distribution system modeling. The mechanisms running hydraulic simulation have been fully developed. However, the simulation of chemical reactions and corrosion are still a major focus in modeling research and development. The further advancement in water quality simulation is being motivated partly by security precautions. The simulation of possibly harmful contaminants in water distribution systems is of major concern for water utilities. To satisfy security demands further research has been conducted in the development of warning system hardware and software.

The simulation of corrosion is still a novel concept and current development has been in the area of identifying corrosion indicators. For example, the accelerated depletion of a disinfectant may indicate that corrosion is forming turbicles on the pipe wall. Once the mechanisms behind pipe corrosion have been fully defined and understood, more advancements will be made in the development of modeling packages.

References

Boccelli, D. L., M. E. Tryby, J. G. Uber and R. S. Summers (2003). "A reactive species model for chlorine decay and THM formation under rechlorination conditions." *Water Research,* 37**,** 2654-2666.

Boulus P. F., Karney B.W., and Lansey K. E. (2006). "Network Components." *Comprehensive Water Distribution Systems Analysis Handbook for Engineers and Planners*, MWH Soft, Pasadena, CA, 3.23-3.25.

Bremond, B., Chesneau, O. and Piller, O. (2003). "Calibration Methodology for a Residual Chlorine Decreasing Model in Drinking Water Networks." *World Water & Environmental Resources Congress*

Bush, C. A. and J. G. Uber (1998). "Sampling design methods for water distribution model calibration." *Journal of Water Resources Planning and Management-Asce,* 124**,** 334-344.

Feinauer, L., Russell, K., and Broadwater, R. (2008). "Graph trace analysis and generic algorithms for interdependent reconfigurable system design and control." *Naval Engineers Journal,* 120**.**

Harding, B. L. and T. M. Walski (2000). "Long time-series simulation of water quality in distribution systems." *Journal of Water Resources Planning and Management-Asce,* 126**,** 199-209.

Huang, J. J. and E. A. McBean (2007). "Using Bayesian statistics to estimate the coefficients of a two-component second-order chlorine bulk decay model for a water distribution system." *Water Research,* 41**,** 287-294.

Mays, L.W. (2004). *Water Supply Systems Security***.** McGraw-Hill, New York, NY.

Meier, R. W. and B. D. Barkdoll (2000). "Sampling design for network model calibration using genetic algorithms." *Journal of Water Resources Planning and Management-Asce,* 126**,** 245-250.

Reddy, P. V. N., K. Sridharan and P. V. Rao (1996). "WLS method for parameter estimation in water distribution networks." *Journal of Water Resources Planning and Management-Asce,* 122**,** 157-164.

Rossman, L. A. and B. F. Boulos (1996). "Numerical methods for modeling water quality in distribution systems: A comparison." *Journal of Water Resources Planning and Management-Asce,* 122**,** 137-146.

Rossman, L. A., R. M. Clark and W. M. Grayman (1994). "Modeling chlorine residuals in drinking-water distribution-systems." *Journal of Environmental Engineering-Asce,* 120**,** 803-820.

Rossman, L.A. (2000) EPANET 2 Users Manuel. Water Supply and Water Resources Division *National Risk Management Research Laboratory.*

Salgado, R., Todini, E. and O'Connell, P.E. (1988). "Comparison of the gradient method with some traditional methods for the analysis of water supply distribution networks."*Computer Applications in Water Supply,* Research Studies Press Ltd. Taunton, UK., 38-62.

Shang, F., J. G. Uber and L. A. Rossman (2008). "Modeling reaction and transport, of multiple species in water distribution systems." *Environmental Science & Technology,* 42**,** 808-814.

Todini, E. and Pilati, S. (1987). "A gradient algorithm for the analysis of pipe networks." *Computer Applications in Water Supply,* Research Studies Press Ltd. Taunton, UK., 1-20.

Usman, A., Powell, R.S. and Sterling, M.J.H. (1988). "Comparison of colebrook-white and hazen-williams flow models in real-time water network simulation." *Computer Applications in Water Supply,* Research Studies Press Ltd. Taunton, UK., 21-37.

Walski, T. M., Chase, D.V., Savic, D.A., Grayman, W., Beckwith, S., and Koelle, E. (2003). *Advanced Water Distribution Modeling and Management.* Haestad Methods, Waterbury, CT.

Zheng, Y. W. (2006). "Optimal calibration method for water distribution water quality model." *Journal of Environmental Science and Health Part a-Toxic/Hazardous Substances & Environmental Engineering,* 41**,** 1363-1378.

Chapter 2: Comparison of EPANET and DEW

2.1 Objectives

Comparing the simulation performance of EPANET and DEW will provide insight into the capabilities of the DEW model. Since EPANET is a well established water distribution system model, it will be considered the standard for the comparison with DEW. The following are the main objectives for this study:

1. The solution methods for DEW, Todini (similar to EPANET solution method), and Hardy-Cross will be used to solve a simple looped network. The hydraulic solutions for the three different methods will be compared. These comparisons will allow for a better understanding of EPANET's and DEW's solution approaches.
2. A simple water distribution network (a different, more complex network from the solution method comparison) will be simulated in both DEW and EPANET. The results of the simulation in both models will be compared and the performance of the DEW model assessed.

Completing the two main objectives as described above will provide valuable information that will be used to better understand the hydraulic solution method in the DEW model. Since DEW is a multi-disciplinary model that is theoretically capable of solving different types of networks (i.e. electrical and water), it is important to assess its ability to perform simple hydraulic simulations. This chapter discusses the comparison of EPANET's and DEW's hydraulic simulation capabilities used as a preliminary assessment of DEW.

2.2 Methodology

Three solution methods were studied by solving a simple looped network with each method. The current DEW solution is an ad-hoc approach that utilizes the bisection method.

The Todini method is very similar to the approach used by EPANET and uses a matrix equation to simultaneously solve for pipe flows and nodal heads. The Hardy-Cross method is a well known and accepted method for network analysis. This method was added to the study due to its similarities with the DEW solution. Both DEW and Hardy-Cross calculate a flow adjustment for each loop, and pipes that are shared by two loops undergo multiple adjustments. The parameters for the simple looped network used in this study remained the same for each method (i.e. pipe length, pipe diameter, pipe roughness, and nodal demands). The number of iterations to convergence and pipe flows were determined for each method and compared. The stopping criteria used for this study was 0.001. This means that when the correction value for both the pipe flows and nodal heads was less than or equal to 0.001, a converged solution was determined.

A simple water distribution network was simulated in both the EPANET and DEW models. Please note that the network used in the model comparison was a different, more complex network from the one used in the solution method comparison. The input parameters for both models were identical (i.e. pipe length, pipe roughness, pipe diameter, nodal demands). The current state of DEW would only allow a steady-state simulation to take place. Therefore, a transient comparison of the two models did not occur. The hydraulic predictions were recorded from both models and compared. Since EPANET is a developed and well accepted hydraulic simulation package, its predictions were held as the correct standard. Thus, taking the results from EPANET as the correct predictions, the comparison allowed for a preliminary assessment of DEW's performance.

2.3 DEW a Graph-Trace Analysis Simulator

DEW is considered a graph trace analysis (GTA) simulator. The concept of GTA is explained in Chapter 1 under section 1.1.3. GTA has been in development for nearly twenty years, and over this period of time has been used to model integrated power transmission and distribution down to the individual consumers for systems composed of millions of components. Theoretically the use of GTA can be extended to any system that can be built as a well-defined network. The real-time monitoring of power, water, gas, and sewage systems has been performed using GTA. The use of GTA allows a modeler to structure and manage common models in addition to performing analyses across multiple system types. Simulations executed by DEW are done through the use of iterators, component objects, system containers and generic algorithms (Feinauer et al. 2008). This is referred to as "Generic Analysis" and is explained in greater detail in Chapter 1 under section 1.1.4.

2.4 Water Analysis in DEW

DEW has the ability to simulate water system hydraulics by the use of the Hazen-Williams, Darcy-Weisbach, or Manning headloss equations. The equations for each method were programmed in DEW and the use of any of the methods is user selectable. The manner in which each equation accounts for pipe roughness is slightly different. The C-factor for the Hazen-Williams equation is looked up by DEW and is determined by the material of the pipe. The Darcy-Weisbach friction factor, f, is a function of the Reynolds number and relative roughness (roughness coefficient divided by the diameter of a pipe) and is determined using the Swamee-Jain equation. Currently in DEW the friction factor is embedded directly into the source code, but will eventually be determined based on pipe material and flow conditions. The Manning roughness, n, is a function of the Reynolds number and the friction factor. This value

is also directly embedded into the source code and not determined for each respective pipe. It is important to note that the DEW model will eventually account for the affects of pipe age on pipe roughness values (i.e. Hazen-Williams C-factor). Due to the current status of DEW, the comparison between EPANET and DEW was performed using the Hazen-Williams equation.

An interesting aspect of the hydraulic solution in DEW is the use of cotrees. A cotree is the result of forming a closed loop within a network. DEW depends on the pressure difference across a cotree for determining convergence. Convergence occurs in DEW when the pressure difference across a cotree is less than a set tolerance. When a system is designed in DEW the first action carried out by the model is determining the feeder path for each component within the system. Once the system is built and the feeder paths defined, the pressures from the sources are propagated to the loads (it is important to note that for the initial propagation the flow is assumed to be zero). At the load components, the initial propagated pressure is used to estimate the flows. Currently in DEW all load components are modeled as constant flow and not pressure dependent, this means that the fluid loads do not depend on the propagated pressure. The flows are then propagated back to the sources using the defined feeder path traces. The flows are next used to estimate the pressure at each component (i.e. a pump curve is used for the pump and a volume curve is used for the tank). The pressure difference is monitored at the cotree. If the difference is not zero or less than a set tolerance, then flow is injected from the high pressure side to the low pressure side. DEW then resets flows using the new cotree pressure difference. This step is repeated until the pressures on both sides of the cotree are equal within a set tolerance.

The prediction of chlorine decay is a major focus for the simulation of water quality in DEW. The first-order reaction of chlorine decay that will be simulated using DEW is described

in Chapter 1 under section 1.2.1. Once the water quality simulation capabilities of DEW have been fully developed, which can only occur once the mechanisms controlling hydraulic simulation have been completely developed, DEW will be able to perform a comprehensive water distribution network simulation.

2.5 Tank Simulation in EPANET and DEW

Tanks in EPANET can be "floating" tanks. "Floating" tanks do not have to be operated manually since they fill and drain by themselves as the head changes due to the diurnal demand. These tanks operate with a given minimum and maximum water level. If the water level during a simulation is lowered below the minimum value, EPANET stops outflow from the tank. Likewise, if the water level exceeds the maximum value, EPANET stops inflow into the tank. EPANET also offers the addition of a volume curve, which allows irregular-shaped tanks to be characterized (if no curve is added, it is assumed that the tank is cylindrical). A source concentration of a chemical (i.e. chlorine) can be an input parameter for a tank so that water flowing into the system from the tank will initially share the same source concentration as the stored tank water. EPANET also offers different mixing models for simulating water quality within the tanks. The mixing models are described as: fully mixed, two-compartment mixing, first-in-first-out plug flow (FIFO), and last-in-first-out plug flow (LIFO). Fully mixed assumes that the water entering the tank instantaneously mixes with the water that is already present within the tank. Two-compartment mixing proposes that there are two zones within the tank. The first zone (inlet-outlet zone) contains the water that is entering and exiting the tank and is being mixed with the water already in that zone. When water "overflows" from the first zone, it then mixes with the water in the main, upper zone. When water is exiting the tank, the water that is released from the inlet-outlet zone is replaced by water from the main zone. The plug flow

mixing models claim that no mixing takes place within the tank and water entering the tank is segregated into parcels that enter and exit in order. The main difference between the two plug flow models, FIFO and LIFO, is that for FIFO the parcels of water enter and exit the tank on the horizontal plane and with LIFO the parcels enter and exit on the vertical plane (Rossman, L.A. 2000).

Currently in DEW, tanks do not behave similarly to "floating" tanks in EPANET. The main difference is that DEW depends on information being transmitted to the model via a SCADA system (Supervisory Control and Data Acquisition). This allows the tank to have a water level that is known in real-time. The drawback to this method is that if a SCADA system cannot be installed into a network, then DEW is unable to account for the rise and fall of the water level in a tank inherent to a distribution system. This approach may be appropriate for real-time simulations where a SCADA system is connected and active, but can be limiting if the model is being used for design purposes. Thus, EPANET treats the water level in a tank as a simulated variable, while DEW treats the water level as an input variable. DEW does, however, share the same ability as EPANET for adding a water quality source for the system being serviced. Mixing within the tank is currently under development and will most likely resemble the aforementioned two-compartment mixing.

2.6 Pump Simulation in EPANET and DEW

Pumps that are functional within an EPANET model depend on the use of a pump curve. A pump curve represents the relationship between pressure head and flow rates that are associated with a pump at its nominal speed setting. A correct pump curve must have a decreasing pressure head with an increasing flow rate. EPANET can use three different pump curves: single-point curve, three-point curve, and multi-point curve. The single-point curve is

formed by defining a single head-flow point that represents the desired operating setting. In this case the rest of the curve is determined by assuming a shut-off head at zero flow equal to 133% of the design head, and a maximum flow at zero head equal to twice the design flow. A three-point curve is formed by defining the low flow (flow and head at low or zero flow condition), design flow (flow and head at desired operating point), and the maximum flow (flow and head at maximum flow) points. With these three points, EPANET fits a continuous function that represents the pump curve. The multi-point curve is formed by entering four or more head-flow points, which EPANET connects with straight line segments forming the pump curve. EPANET is also able to simulate variable speed pumps. In this scenario the pump curve shifts as the speed of the pump changes. The following are the relationships of flow (Q) and head (H) to speeds N_1 and N_2 (Rossman, L.A. 2000):

$$\frac{Q_1}{Q_2} = \frac{N_1}{N_2} \qquad \text{Eq. 2.1}$$

$$\frac{H_1}{H_2} = \left(\frac{N_1}{N_2}\right)^2 \qquad \text{Eq. 2.2}$$

If the system requires a head that is greater than the first point on the pump curve, then EPANET will shut down the pump (this is known as the shut-off head).

Currently in DEW, pumps do not have the capability to operate with pump curves. As of now, the model treats pumps as a constant pressure source. Thus, a pump would depend on a SCADA system to relay the current pressure of the corresponding pump in the network. This method does not allow DEW to properly simulate a pump's behavior in a network that does not have a SCADA system. The use of a pump curve is under development, but may not have the same functionality as in EPANET.

2.7 Solution Method Comparison

Three different solution methods were used to perform hydraulic calculations for a simple looped network (Figure 2.1 below). The three methods are the Todini (gradient method), Hardy-Cross, and DEW solution method. The Hardy-Cross solution method was included in the comparison because like DEW, it calculates an adjustment for each loop (cotree), and pipes common to more than one loop undergo multiple adjustments. The input parameters remained constant for each method so that a meaningful comparison could be made. The following figure and tables contain the simple looped network and parameters respectively for the solution method comparison:

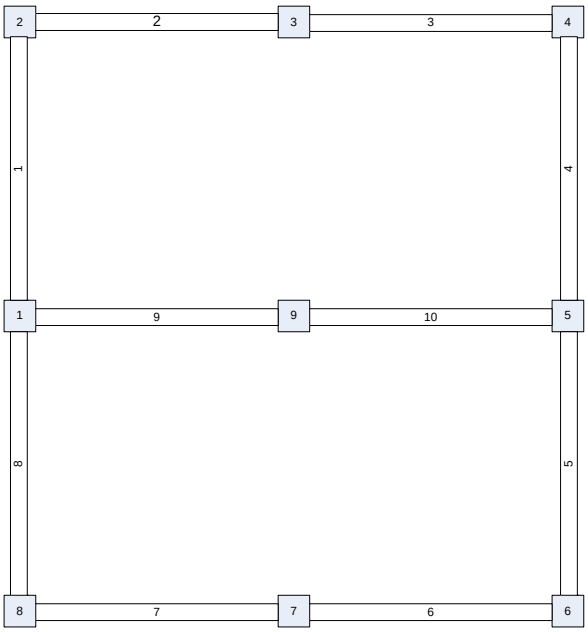

Figure 2.1: Solution Comparison Network

Table 2.1: Pipe Parameters

Link	Diameter	Length	C-Factor
	(in)	(ft)	
1	6	2000	100
2	6	1000	100
3	6	1000	100
4	6	2000	100
5	6	2000	100
6	6	1000	100
7	6	1000	100
8	6	2000	100
9	6	2000	100
10	6	2000	100

Table 2.2: Nodal Demands & Sources

Node	Nodal Demand	Nodal Source
	(gpm)	(gpm)
1	0	0
2	0	0
3	0	0
4	200	0
5	0	600
6	400	0
7	0	0
8	400	0
9	600	0

** Node 1 was set as a fixed head of 219.05 ft (100 psi)*

The Todini method is also known as the gradient method and is very similar to the approach used by EPANET. This method uses matrices that contain a set of *npipe* and *nnode* equations to equal the number of unknowns. The matrix solution is in the form of (Todini et al. 1987):

$$\begin{matrix} & npipe & nnode \\ npipe \\ nnode \end{matrix} \begin{bmatrix} nA_{11} & A_{12} \\ A_{21} & 0 \end{bmatrix} \begin{bmatrix} dQ \\ - - \\ dH \end{bmatrix} = \begin{bmatrix} -dE \\ - - \\ -dq \end{bmatrix} \qquad \text{Eq. 2.3}$$

Where:

n = Value based on which head-loss equation used (i.e. 1.852 for Hazen-Williams)

nA_{11} = Matrix comprised of the derivatives with respect to pipe flow = $nK|Q|^{n-1}$

K = $K_u \frac{L}{D^{4.87} C_{HW}^n}$

K_u = Unit constant (i.e. 10.57 for English units: D-L-Q in in, ft, gpm)

A_{21} = Connectivity (topological) matrix

A_{12} = Transpose of matrix A_{21}

dQ = Change in pipe flow (L^3/T)

dH = Change in nodal head (L)

-dE = Pipe balance error (L)

-dq = Nodal balance error (L^3/T)

Please note that in equation 2.3 above, the "*npipe*" and "*nnode*" labels signify how the sizes of the matrices depend on the number of pipes and nodes in a system (i.e. nA_{11} is a square npipe x npipe matrix). The result of the nA_{11}, A_{21}, A_{12}, and 0 matrices combined is essentially a Jacobian matrix for the system and will be identified as the A matrix. The following figure shows the initial flow magnitudes and directions in the sample network used for the Todini method:

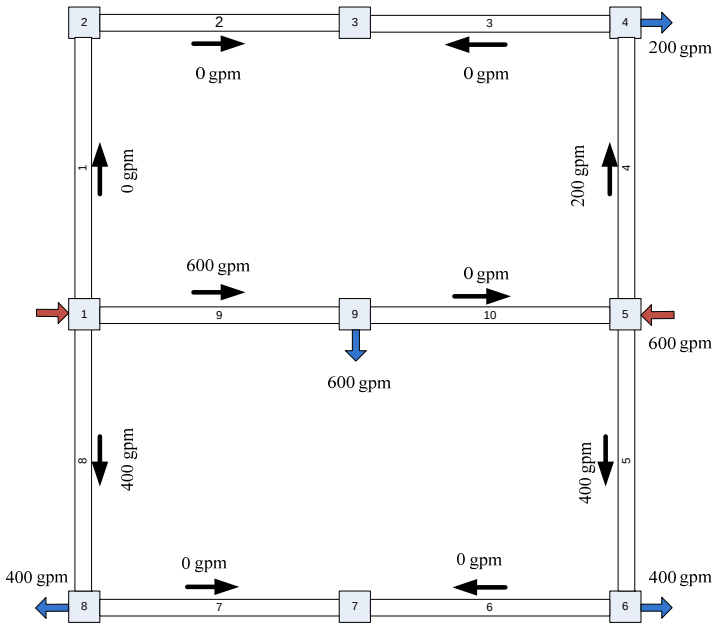

Figure 2.2: Initial Flow Magnitudes & Directions for Todini Approach

Please note, that in Figure 2.2 the black arrows denote the flow directions, the blue arrows represent nodal demands, and the red arrows represent sources. The solution for the Todini method for the example network in Figure 2.2 can be found in the Appendix. The following figure is the first iteration for the Todini solution:

ITERATION 1			1	2	3	4	5	6	7	8	9	10	2	3	4	5	6	7	8	9	
index	Q0 | H0		AUGMENTED A																		RHS
1	0		0	0	0	0	0	0	0	0	0	0	1	0	0	0	0	0	0	0	129.048
2	0		0	0	0	0	0	0	0	0	0	0	-1	1	0	0	0	0	0	0	0
3	0		0	0	0	0	0	0	0	0	0	0	0	1	-1	0	0	0	0	0	0
4	200		0	0	0	0.115	0	0	0	0	0	0	0	0	1	-1	0	0	0	0	-12.3662
5	400		0	0	0	0	0.207	0	0	0	0	0	0	0	0	-1	1	0	0	0	-44.6422
6	0		0	0	0	0	0	0	0	0	0	0	0	0	0	0	-1	1	0	0	0
7	0		0	0	0	0	0	0	0	0	0	0	0	0	0	0	0	1	-1	0	0
8	400		0	0	0	0	0	0	0	0.207	0	0	0	0	0	0	0	0	1	0	84.4054
9	600		0	0	0	0	0	0	0	0	0.292	0	0	0	0	0	0	0	0	1	34.453
10	0		0	0	0	0	0	0	0	0	0	0	0	0	0	1	0	0	0	-1	0
2	90		1	-1	0	0	0	0	0	0	0	0	0	0	0	0	0	0	0	0	0
3	90		0	1	1	0	0	0	0	0	0	0	0	0	0	0	0	0	0	0	0
4	90		0	0	-1	1	0	0	0	0	0	0	0	0	0	0	0	0	0	0	0
5	90		0	0	0	-1	-1	0	0	0	0	1	0	0	0	0	0	0	0	0	0
6	90		0	0	0	0	1	-1	0	0	0	0	0	0	0	0	0	0	0	0	0
7	90		0	0	0	0	0	1	1	0	0	0	0	0	0	0	0	0	0	0	0
8	90		0	0	0	0	0	0	-1	1	0	0	0	0	0	0	0	0	0	0	0
9	90		0	0	0	0	0	0	0	0	1	-1	0	0	0	0	0	0	0	0	0

Figure 2.3: First Iteration for Todini Method

When referring to the first iteration above, cell (1, 1) in the nA_{11} portion (pink segment in Figure 2.3) of the A matrix represents pipe 1, cell (2, 2) refers to pipe 2, cell (3,3) refers to pipe 3, and so on. The first iteration for the solution uses the initial guesses for pipe flow and direction (a flow balance for the network is not a requirement). The following is an example calculation for the value corresponding to pipe 4, cell (4, 4), in the nA_{11} portion of the matrix above:

$$nK|Q|^{n-1} = 1.852 * 10.57 * \frac{2000\ ft}{((6\ in)^{4.87})(100^{1.852})} * (200\ gpm)^{1.852-1} = 0.115$$

In the A_{21} portion (blue segment in Figure 2.3) of the A matrix, the connectivity among the nodes and pipes are defined. For instance, the first row in the A_{21} portion represents node 2 and its connectivity with the pipes. It is important to note that node 1 is not included in the matrix because it is a constant known head. Each cell in the row accounts for each pipe, the first cell in the first row accounts for the connectivity of node 2 with pipe 1, the second cell in the first row accounts for the connectivity of node 2 with pipe 2, and so on. The derivatives with

respect to the nodal heads are 0, 1, or -1. A 0 is used when a pipe is not connected to a node, a 1 is used if a pipe is connected to a node and the flow enters the node (sink node), and a -1 is used when a pipe is connected to a node but the flow is exiting the node (source node). Therefore, the row corresponding to node 2 has a 1 and -1 in the first two cells and 0's in the remaining cells. This is because pipe 1 has flow entering node 2 and pipe 2 has flow exiting node 2, and the rest of the pipes are not connected to node 2 and thus are assigned a value of 0. The remaining cells in the A matrix are simply the transpose of A_{21} (the A_{12} section, light green segment) and a 0 matrix.

The right side of the solution, $\begin{bmatrix} -dE \\ -- \\ -dq \end{bmatrix}$, accounts for the pipe balance error (-dE) and the nodal balance error (-dq). The pipe balance error is essentially an energy balance through a pipe. Thus, -dE can be defined by the following equation (Todini et al 1987):

$$-dE = -(K_i Q_i^n + H_2 - H_1) \qquad \text{Eq. 2.4}$$

Where:

$K_i Q_i^n$ = Head-loss through a pipe (Hazen-Williams) (L)

$K_i = K_u \frac{L}{D^{4.87} C_{HW}^n}$ (Hazen-Williams)

K_u = Unit constant (i.e. 10.57 for English units: D-L-Q in in, ft, gpm)

H_2 = Head at downstream node (L)

H_1 = Head at upstream node (L)

For instance, the pipe balance error for pipe 1in the first iteration based on the initial flow estimates is: –(0.0007*0^1.852 + 90 -219.048) = 129.048 ft.

The nodal balance error is essentially a flow balance at a node. Thus, -dq can be defined by the following equation (node 4 is used) (Todini et al. 1987):

$$-dq_4 = -(-Q_3 + Q_4 - q_4) \qquad \text{Eq. 2.5}$$

Where:

Q_3 = Flow through pipe 3 (L^3/T)

Q_4 = Flow through pipe 4 (L^3/T)

q_4 = Demand at node 4 (L^3/T)

Therefore, for node 4 the nodal balance error is –(-0+200-200) = 0 gpm. Please note that the example calculation performed above are from the first iteration of the solution (Figure 2.3). With the A matrix and balance error matrix determined, the change in flow/head matrix, $\begin{bmatrix} dQ \\ -- \\ dH \end{bmatrix}$, can be determined. The change in flow/head matrix is determined by multiplying the inverse of the A matrix by the balance error matrix, as demonstrated in the following figure:

1	2	3	4	5	6	7	8	9	10	2	3	4	5	6	7	8	9					
A INVERSE																			RHS		dQ | dH
3.501	3.501	-3.501	-3.501	1.449	1.449	-1.449	-1.449	-2.052	-2.052	1.000	1.000	1.000	0.599	0.300	0.300	0.300	0.599		129.0476		237.3847
3.501	3.501	-3.501	-3.501	1.449	1.449	-1.449	-1.449	-2.052	-2.052	0.000	1.000	1.000	0.599	0.300	0.300	0.300	0.599		0		237.3847
-3.501	-3.501	3.501	3.501	-1.449	-1.449	1.449	1.449	2.052	2.052	0.000	0.000	-1.000	-0.599	-0.300	-0.300	-0.300	-0.599		0		-237.385
-3.501	-3.501	3.501	3.501	-1.449	-1.449	1.449	1.449	2.052	2.052	0.000	0.000	0.000	-0.599	-0.300	-0.300	-0.300	-0.599		-12.3662		-237.385
1.449	1.449	-1.449	-1.449	2.018	2.018	-2.018	-2.018	0.568	0.568	0.000	0.000	0.000	-0.166	0.417	0.417	0.417	-0.166		-44.6422		-35.843
1.449	1.449	-1.449	-1.449	2.018	2.018	-2.018	-2.018	0.568	0.568	0.000	0.000	0.000	-0.166	-0.583	0.417	0.417	-0.166		0		-35.843
-1.449	-1.449	1.449	1.449	-2.018	-2.018	2.018	2.018	-0.568	-0.568	0.000	0.000	0.000	0.166	0.583	0.583	-0.417	0.166		0		35.84301
-1.449	-1.449	1.449	1.449	-2.018	-2.018	2.018	2.018	-0.568	-0.568	0.000	0.000	0.000	0.166	0.583	0.583	0.583	0.166	x	84.40544	=	35.84301
-2.052	-2.052	2.052	2.052	0.568	0.568	-0.568	-0.568	2.620	2.620	0.000	0.000	0.000	0.235	0.117	0.117	0.117	0.235		34.45302		-273.228
-2.052	-2.052	2.052	2.052	0.568	0.568	-0.568	-0.568	2.620	2.620	0.000	0.000	0.000	0.235	0.117	0.117	0.117	-0.765		0		-273.228
1.000	0.000	0.000	0.000	0.000	0.000	0.000	0.000	0.000	0.000	0.000	0.000	0.000	0.000	0.000	0.000	0.000	0.000		0		129.0476
1.000	1.000	0.000	0.000	0.000	0.000	0.000	0.000	0.000	0.000	0.000	0.000	0.000	0.000	0.000	0.000	0.000	0.000		0		129.0476
1.000	1.000	-1.000	0.000	0.000	0.000	0.000	0.000	0.000	0.000	0.000	0.000	0.000	0.000	0.000	0.000	0.000	0.000		0		129.0476
0.599	0.599	-0.599	-0.599	-0.166	-0.166	0.166	0.166	0.235	0.235	0.000	0.000	0.000	-0.069	-0.034	-0.034	-0.034	-0.069		0		114.2306
0.300	0.300	-0.300	-0.300	0.417	-0.583	0.583	0.583	0.117	0.117	0.000	0.000	0.000	-0.034	-0.120	-0.120	-0.120	-0.034		0		76.99693
0.300	0.300	-0.300	-0.300	0.417	0.417	0.583	0.583	0.117	0.117	0.000	0.000	0.000	-0.034	-0.120	-0.120	-0.120	-0.034		0		76.99693
0.300	0.300	-0.300	-0.300	0.417	0.417	-0.417	0.583	0.117	0.117	0.000	0.000	0.000	-0.034	-0.120	-0.120	-0.120	-0.034		0		76.99693
0.599	0.599	-0.599	-0.599	-0.166	-0.166	0.166	0.166	0.235	-0.765	0.000	0.000	0.000	-0.069	-0.034	-0.034	-0.034	-0.069		0		114.2306

Figure 2.4: Solution of First Iteration for Todini Method

Once the change vector is determined the initial flow and head values are corrected and the next iteration is performed. This continues until the changes in flow and head are less than a certain tolerance.

The Hardy-Cross approach is a well known and understood method that solves the energy equations for loops and pseudo-loops for a loop-flow correction. This method solves one loop at

a time, in that one loop equation is written for each closed loop. It is important to note that for this method a flow balance must be made in the system before the first iteration (initial flow directions do not have to be correct). The Hardy-Cross approach is described in detail in Chapter 1 under section 1.1.2. The following figure shows the initial flow magnitudes and directions for the Hardy-Cross method:

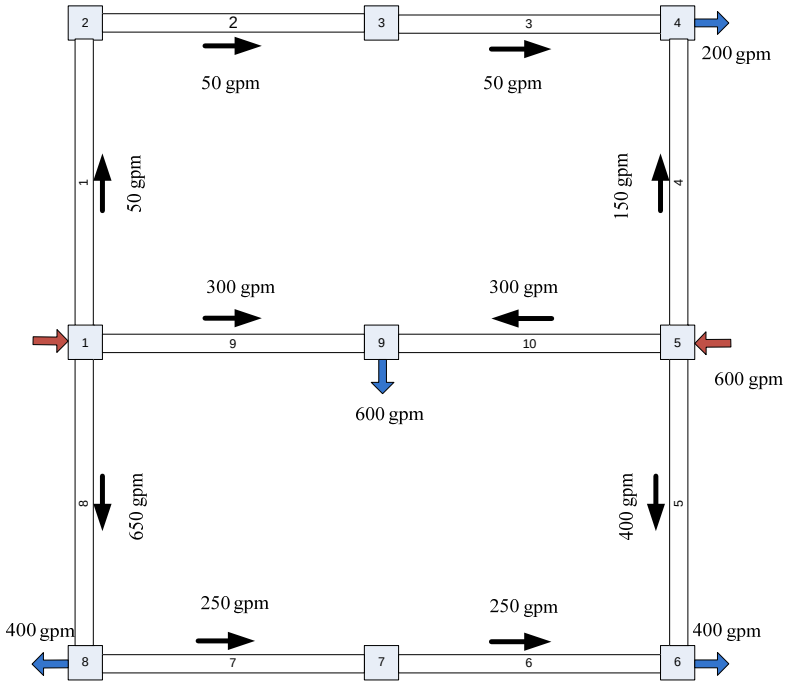

Figure 2.5: Initial Flow Magnitudes & Directions for Hardy-Cross Method

As stated before, this flow correction is applied to every pipe within the closed loop of interest. The value of ΔQ_{LP} (flow correction for a loop) determines whether or not the solution proceeds to another iteration. If the value of ΔQ_{LP} is less than a specified tolerance then the solution stops and if it is not the solution continues through another iteration. This method was used to solve the example looped network in Figure 2.5. For this solution it is important to note that pipes 9 and 10 are shared between both loops. This means that pipes 9 and 10 will have two

flow corrections applied for each iteration (one from the top loop and one from the bottom loop). The entire solution for this method can be found in the Appendix. This solution uses the Hazen-Williams head-loss equation for determining the loop equations and flow corrections. To illustrate the point made about pipes 9 and 10, refer to the first iteration in the solution, which is given in the following figure:

ITERATION 1						
Link	Diam	Length	Flow	hL	hL/Q	New Flow
	in	ft	gpm	ft	ft/gpm	gpm
1	6	2000	50	0.950607	0.019012	61.10
2	6	1000	50	0.475303	0.009506	61.10
3	6	1000	50	0.475303	0.009506	61.10
4	6	2000	-150	-7.27159	0.048477	-138.90
10	6	2000	300	26.25046	0.087502	311.10
9	6	2000	-300	-26.2505	0.087502	-288.90
			SUM	-5.37038	0.261505	
			DELTA Q	11.1008		
9	6	2000	288.9	24.47996	0.084735	433.39
10	6	2000	-311.1	-28.0777	0.090253	-166.61
5	6	2000	150	7.27159	0.048477	294.50
6	6	1000	-250	-9.36404	0.037456	-105.50
7	6	1000	-250	-9.36404	0.037456	-105.50
8	6	2000	-650	-109.907	0.169087	-505.50
			SUM	-124.961	0.467465	
			DELTA Q	144.4952		

Figure 2.6: First Iteration for Hardy-Cross Solution

For the top loop (pipes 1=>2=>3=>4=>10=>9), where clockwise is the positive direction, the ΔQ_{LP} applied to every pipe is 11.1 gpm. As a result, the corrected flows through pipes 9 and 10 from the top loop are -288.90 and 311.10 gpm respectively. These corrected values are then used as the initial flows for the bottom loop (still within the first iteration). Based on the sign convention the direction of flow is reversed for pipes 9 and 10 in the bottom loop. Thus the flows through pipes 9 and 10 in the bottom loop are 288.90 and -311.10 gpm respectively. The

ΔQ_{LP} for the bottom loop is 144.5 gpm, thus the corrected flows for pipes 9 and 10 for the first iteration are 433.39 and -166.61 gpm respectively.

The current DEW solution method can be considered a modified Hardy-Cross approach. This is because DEW performs an energy balance across a loop in a manner very similar to the Hardy-Cross method and both methods attempt to make the sum of the pressures across a loop equal to zero. A major difference is that DEW uses cotrees as the point where a closed loop is monitored. Additionally, DEW solves each cotree individually which is the same as Hardy-Cross solving each loop individually. DEW performs a radial solution for a loop from both sides of the cotree and determines the pressure difference from both sides of the loop at the cotree. The DEW solution for the sample network in Figure 2.7 (below) utilizes graph trace analysis to perform the calculations. The following figure shows the initial flow magnitudes and directions for the DEW solution:

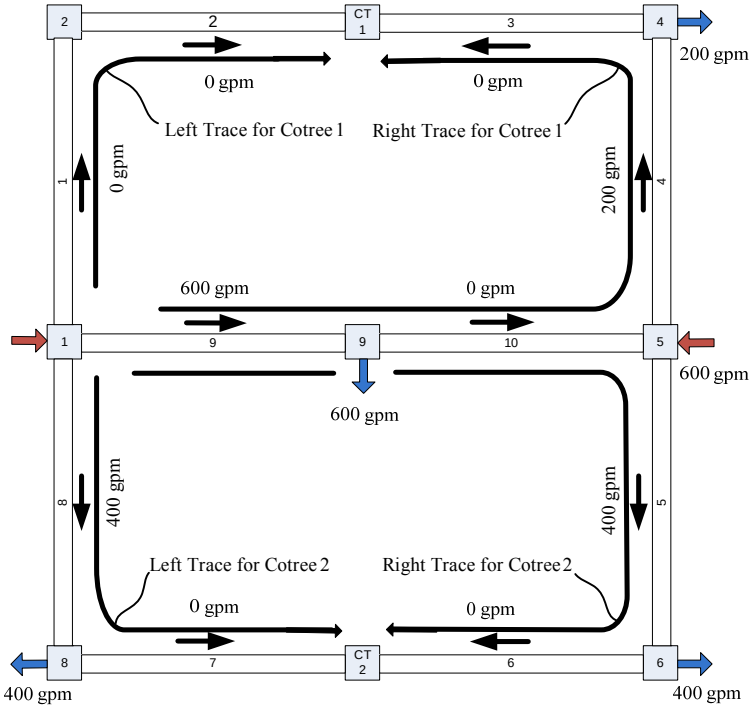

** CT 1and CT 2 are the locations of cotree 1 and cotree 2 respectively*

Figure 2.7: Initial Flow Magnitudes & Directions for DEW Solution

Hazen-Williams is the head-loss equation used for this solution. The first part of this solution (DEW solution is found in the Appendix) is performing a flow balance; DEW performs a flow balance that simply satisfies the demands at nodes 4, 6, 8, and 9. For the first iteration DEW checks the change in pressure across the cotrees for the top and bottom loops (CT 1 and CT 2 are the locations of the cotrees for the top and bottom loops respectively). The top loop is comprised of pipes 1 and 2 for the left side of the cotree and pipes 9, 10, 4, and 3 for the right side of the cotree. The bottom loop is comprised of pipes 8 and 7 for the left side of the cotree and pipes 9, 10, 5, and 6 for the right side of the cotree. For the second iteration DEW adds flow to the loop that contains the cotree with the larger pressure difference from the first iteration (the top loop in this example). The flow is added to the side of the cotree with the larger pressure so that flow goes in the direction of high pressure to low pressure. The following figure contains the first and second iterations from the DEW solution:

Iteration 1				
Pipe ID	Flow (gpm)	Length (ft)	hf (ft)	psi
1	0	2000	0.00	0.00
2	0	1000	0.00	0.00
3	0	1000	0.00	0.00
4	200	2000	12.39	5.37
5	400	2000	44.72	19.38
6	0	1000	0.00	0.00
7	0	1000	0.00	0.00
8	400	2000	44.72	19.38
9	600	2000	94.76	41.06
10	0	2000	0.00	0.00

cotree 1 Δp = (100-(0+0))-(100-(41.06+0+5.37+0)) = 46.43 psi
cotree 2 Δp = (100-(19.38+0))-(100-(41.06+0+19.38+0)) = 41.06 psi

Iteration 2				
Pipe ID	Flow (gpm)	Length (ft)	hf (ft)	psi
1	71.9	2000	1.86	0.81
2	71.9	1000	0.93	0.40
3	71.9	1000	0.93	0.40
4	128.1	2000	5.43	2.35
5	400	2000	44.72	19.38
6	0	1000	0.00	0.00
7	0	1000	0.00	0.00
8	400	2000	44.72	19.38
9	528.1	2000	74.81	32.42
10	71.9	2000	1.86	0.81

cotree 1 Δp = (100-(0.81+0.40))-(100-(32.42-0.81+2.35-0.40)) = 32.35 psi
cotree 2 Δp = (100-(19.38+0))-(100-(32.42-0.81+19.38+0)) = 31.61 psi

Figure 2.8: First and Second Iterations of the DEW Solution

It is important to note that DEW currently uses a flow correction that remains constant for every iteration and is user defined (71.9 gpm for this solution). Using the corrected flows DEW performs the same actions as in the first iteration and compares the pressure difference across the cotrees. This continues until the change in pressure across the cotrees switch from positive to negative or vice versa. At this point, the change in flow supplied to a particular loop is reduced by half. This is where DEW is utilizing the bisection method to converge on a solution. DEW terminates this method once the pressure differences across the cotrees are zero or less than some tolerance. The DEW solution uses an ad-hoc version of this bisection method. Currently DEW is programmed so that the bisection method initiates only if the current cotree being solved stays constant for the next iteration (i.e. the same cotree has the largest pressure

difference) and the sign of the pressure difference across that cotree changes. For this example the DEW solution first used this bisection method in the eighth iteration for the lower cotree (cotree 2). The following figure contains the sixth, seventh, and eighth iteration for the DEW method:

Iteration 6				
Pipe ID	Flow (gpm)	Length (ft)	hf (ft)	Pressure (psi)
1	215.7	2000	14.25	6.17
2	215.7	1000	7.12	3.09
3	215.7	1000	7.12	3.09
4	15.7	2000	0.11	0.05
5	400	2000	44.72	19.38
6	0	1000	0.00	0.00
7	0	1000	0.00	0.00
8	400	2000	44.72	19.38
9	384.3	2000	41.53	17.99
10	215.7	2000	14.25	6.17

cotree 1 Δp = (100-(6.17+3.09))-(100-(17.99-6.17-0.05-3.09)) = -0.578 psi
cotree 2 Δp = (100-(19.38+0))-(100-(17.99-6.17+19.38-0)) =11.819 psi

Iteration 7				
Pipe ID	Flow (gpm)	Length (ft)	hf (ft)	Pressure (psi)
1	179.7	2000	10.16	4.40
2	179.7	1000	5.08	2.20
3	179.7	1000	5.08	2.20
4	20.3	2000	0.18	0.08
5	328.1	2000	30.99	13.43
6	71.9	1000	0.93	0.40
7	71.9	1000	0.93	0.40
8	471.9	2000	60.74	26.32
9	348.4	2000	34.63	15.01
10	251.6	2000	18.95	8.21

cotree 1 Δp = (100-(4.40+2.20))-(100-(15.01-8.21+0.08-2.20)) = -1.935 psi
cotree 2 Δp = (100-(26.32+0.40))-(100-(15.01-8.21+13.43-0.40)) =-6.907psi

Iteration 8				
Pipe ID	Flow (gpm)	Length (ft)	hf (ft)	Pressure (psi)
1	179.7	2000	10.16	4.40
2	179.7	1000	5.08	2.20
3	179.7	1000	5.08	2.20
4	20.3	2000	0.18	0.08
5	364.1	2000	37.57	16.28
6	35.9	1000	0.26	0.11
7	35.9	1000	0.26	0.11
8	435.9	2000	52.44	22.72
9	384.3	2000	41.53	17.99
10	215.7	2000	14.25	6.17

Figure 2.9: Iterations Six through Eight for the DEW Solution

The bisection method was used in the eighth iteration because the lower cotree (cotree 2) remained constant from the sixth to seventh iteration and the sign of the pressure difference changed. For the seventh iteration a correction of 71.9 gpm was used for the lower loop and for the eighth iteration that correction was divided by two making it 35.9 gpm.

As previously noted, DEW uses a constant flow correction that is applied throughout the solution. This technique does not optimize the solution method since the predefined correction value is not determined at each iteration, making it more difficult to converge on a solution. Thus, it would be advantageous to use a technique that determines a correction value for each iteration. This could be performed by using the Hardy-Cross method. However, the Hardy-Cross method can only work if there is flow going through all of the pipes. If there is a pipe within a loop that has no flow than the solution will not work (h_L/Q = Not Defined). Perhaps the Hardy-Cross method could be used once DEW has simulated flow into all of the pipes using the predefined correction value. Once pipes have flow, using the Hardy-Cross solution could potentially prove to be beneficial to the DEW solution.

The converged values for the simple network from all three of the solution methods were compared. When comparing the solution methods, it is evident that the Todini method (gradient approach) converged on a solution in the fewest number of iterations. The solution shows that by the fifth iteration the change in the flow/head vector contain values that were less than the predefined stopping criteria of 0.001. The Hardy-Cross solution converged on a solution at the eleventh iteration where the change in flow for both loops was less than or equal to the stopping criteria of 0.001. After allowing the DEW model to run to completion, it converged on a solution that is very similar to the Todini approach. To illustrate the number of iterations

required for DEW to converge in comparison to the Todini method, a plot (Figure 2.10 below) was made for the flow estimate for pipe 4 at each iteration.

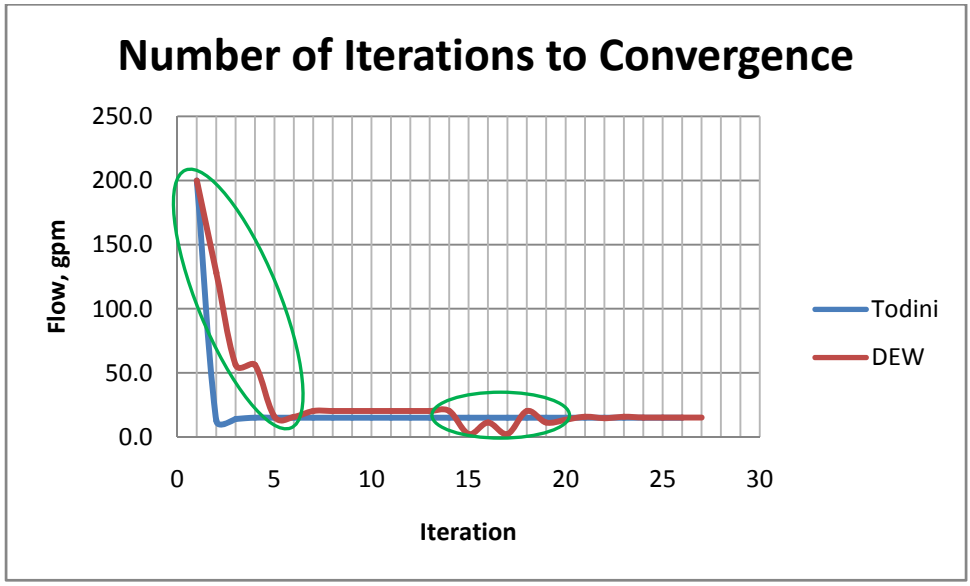

Figure 2.10: Number of Iterations for Pipe 4 for Todini and DEW Methods

According to Figure 2.10 it appears that the Todini method converged on a flow value by the fourth iteration, whereas the DEW solution converged on a flow value around the twenty-fifth iteration. Figure 2.10 also shows that the DEW solution fluctuated from what appears to be a converged solution between the fourteenth and twentieth iterations. This fluctuation is most likely due to the fact that DEW attempts to solve each loop (cotree) individually, and can inadvertently readjust a cotree that has satisfied the convergence criteria. Thus, the fluctuation from a converged solution could have been caused by an adjustment made on one of the cotrees that adversely affected the estimate through the other. However, it is important to note that in Figure 2.10, the portions of the red line enclosed in the green circles indicate when cotree 1 (CT 1) was being solved by DEW. This is known because pipe 4 is associated with CT 1 and the estimated flow fluctuated when the flow through CT 1 was adjusted. Each iteration of the Todini

method is rather extensive (solving the whole system) when compared to the DEW approach, which explains why the Todini solution converged in less iterations. Figure 2.10 shows that the two methods converged on a flow value through pipe 4 that is approximately the same. The bisection method is being used by DEW because it will eventually converge on a solution. This is supported by the results from DEW and how they compare to the Todini method. The DEW method took longer, but it eventually converged on practically the same flow values as the Todini method. Table 2.3 contains the flow values for each pipe for all three solution methods:

Table 2.3: Results for Solution Comparison

	Flow (gpm)		
Pipe	Todini	DEW	Hardy-Cross
1	184.9	184.9	184.9
2	184.9	184.9	184.9
3	184.9	184.9	184.9
4	15.1	15.1	15.1
5	350.7	350.8	350.8
6	49.3	49.2	49.3
7	49.3	49.2	49.3
8	449.3	449.2	449.3
9	365.8	365.9	365.9
10	234.2	234.1	234.2

**Todini converged in 5 iterations, H-C converged in 11 iterations, DEW converged in 25 iterations*

A root mean square value was determined for the following flow estimate comparisons: Todini/DEW, Todini/H-C, and DEW/H-C. A root mean square value of 0.08, 0.04, and 0.06 gpm was calculated for the Todini/DEW, Todini/H-C, and DEW/H-C comparisons respectively. The root mean square values represent the average difference in flow for each comparison. These values indicate that all three methods resulted in flow predictions that were very close in value.

The solution method for DEW is based on a multidisciplinary approach that has been in development for nearly twenty years for use in electrical power systems. Currently DEW has been successful in simulating several types of electrical distribution and transmission networks which traditionally require the use of different approaches. This means that the same solution method could be used for electrical, water, sewer, and gas. This method utilizes GTA to store information about the system and to solve network parameters.

2.8 DEW and EPANET Model Simulation Comparison

A simple looped network (Figure 2.11) was simulated in DEW and EPANET. The input parameters for the network remained identical for both models. All of the pipes in the system had a length of 500 feet and a Hazen-Williams C-factor of 130. The diameters of the pipes varied and can be found under Table 2.5. The elevations of every node in the system remained the same and the demands varied with magnitudes found in Table 2.4. There were two tanks (T1 and T2) in the network, each held at a constant pressure head of 236 feet. Due to the history and acceptance of EPANET, the results from its simulation were considered the correct values.

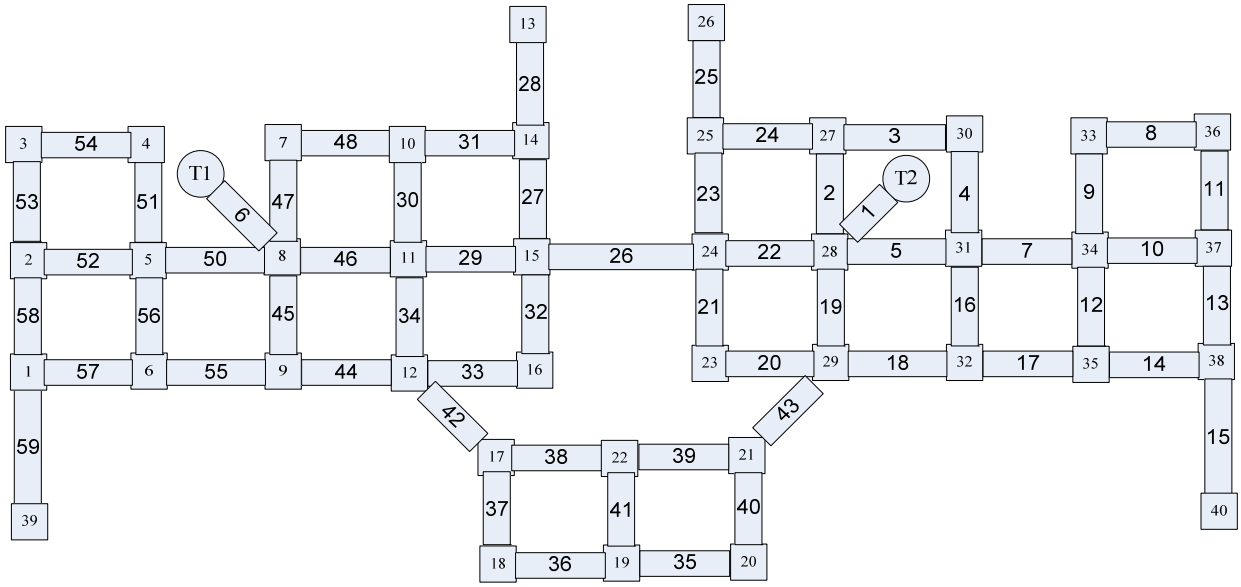

Figure 2.11: Simple Looped Network Used for Model Comparison

Table 2.4: Nodal Demands

Node	Demand (gpm)
1	5.79
2	5.79
3	5.79
4	5.79
5	5.79
6	5.79
7	11.57
8	11.57
9	11.57
10	11.57
11	11.57
12	11.57
13	11.57
14	11.57
15	11.57
16	11.57
17	5.79
18	5.79
19	5.79
20	5.79
21	5.79
22	5.79
23	11.57
24	11.57
25	11.57
26	11.57
27	11.57
28	11.57
29	11.57
30	11.57
31	11.57
32	11.57
33	5.79
34	5.79
35	5.79
36	5.79
37	5.79
38	5.79
39	5.79
40	5.79

Table 2.5: Pipe Parameters

Pipe ID	Length (ft)	Diameter (in)
1	500	12
2	500	6
3	500	6
4	500	6
5	500	8
6	500	12
7	500	4
8	500	4
9	500	4
10	500	4
11	500	4
12	500	4
13	500	4
14	500	4
15	500	4
16	500	6
17	500	4
18	500	6
19	500	6
20	500	6
21	500	6
22	500	8
23	500	6
24	500	6
25	500	6
26	500	8
27	500	6
28	500	6
29	500	8
30	500	6
31	500	6
32	500	6
33	500	6
34	500	6
35	500	4
36	500	4
37	500	4
38	500	4
39	500	4
40	500	4
41	500	12
42	500	4
43	500	4
44	500	6
45	500	6
46	500	8
47	500	6
48	500	6
50	500	4
51	500	4
52	500	4
53	500	4
54	500	4
55	500	4
56	500	4
57	500	4
58	500	4
59	500	4

The simulation in both DEW and EPANET was steady-state and solved using the Hazen-Williams equation. Due to the current state of DEW, a transient analysis comparison could not be performed. The results for the flow through the pipes can be found under Table 2.6. The default maximum number of iterations for DEW is one-thousand. To simply ensure that DEW did not reach its maximum number of iterations before a converged solution was determined, the value was increased to one-hundred-thousand. The first attempt of simulating the network in DEW resulted in relatively different flow values from EPANET. Additionally, the flow directions for pipes 30, 31, and 33 were in the opposite direction from EPANET. The different flow directions caused a greater difference in the flow values between DEW and EPANET in the affected pipes. A possible reason for the different flow directions was the set tolerance value in DEW. This tolerance value is the level at which DEW interprets the pressure difference at the cotrees. If the tolerance value is too high, then DEW does not have a strict stopping criterion for convergence. DEW has a default tolerance value of 0.001, which can be manually adjusted. The first simulation with DEW already had an adjusted tolerance value of $1x10^{-4}$. To test whether the tolerance value would affect the results from DEW, it was changed from $1x10^{-4}$ to $1x10^{-6}$ and the simulation was rerun. With the new tolerance value, the simulated flow values from DEW were very close in comparison to EPANET. This indicates that the stopping criterion had a large influence on the performance of DEW. Additionally, DEW converged on a solution because it satisfied the tolerance value at each cotree and did not reach the maximum number of iterations.

Two root mean square values were calculated for the EPANET and DEW flow estimates, one for each tolerance value in DEW. The root mean square value that corresponds to the comparison between EPANET and DEW at a tolerance of $1x10^{-4}$ is 4.1 gpm. Whereas, the root mean square value that corresponds to the comparison with a DEW tolerance of $1x10^{-6}$ is 0.028

gpm. These values indicate that the flow estimates determined by EPANET and DEW are much closer when DEW was set with a tolerance value of $1x10^{-6}$. Figure 2.12 below contains a graphical comparison of the simulated flows for EPANET and DEW with a tolerance value of $1x10^{-6}$. This figure indicates that the predicted flow values from EPANET and DEW (tolerance value of $1x10^{-6}$) are effectively the same. This is supported by the fitted line with a slope of 1 and an R^2 value of 1.

The simulation run times for EPANET and DEW were relatively the same. Both models completed the simulation in approximately one second. However, a greater distinction in time could be present if the models were simulating a much larger network. Please note that the nodal pressures were the same when DEW had a tolerance of $1x10^{-6}$. It is important to note that the default stopping criteria for EPANET is 0.001. This value was not adjusted for the comparison with DEW.

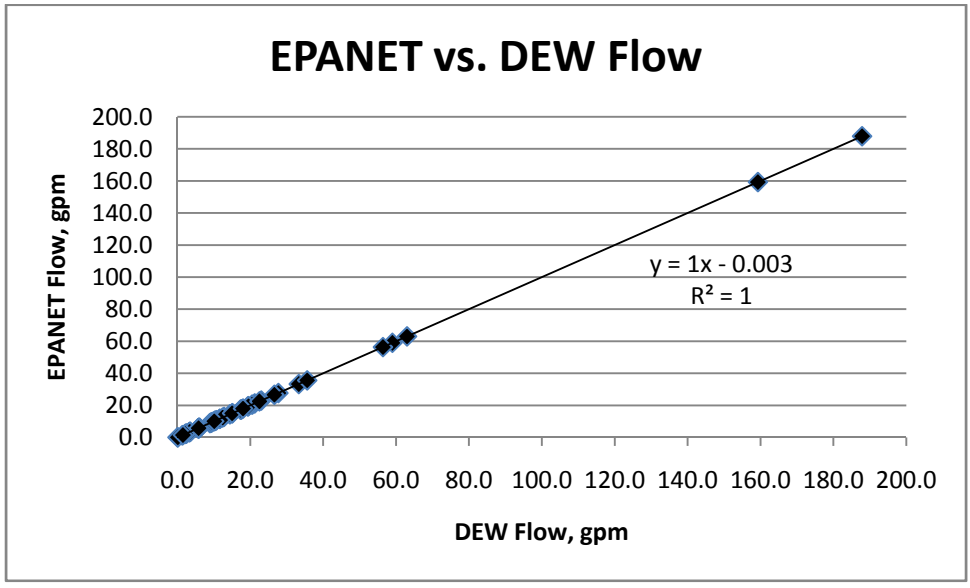

Figure 2.12: Simulated Flows for EPANET and DEW with a Tolerance of $1x10^{-6}$

Table 2.6: DEW/EPANET Comparison Results

	Flow (gpm)		
Pipe ID	EPANET	DEW (Tol = 1e-4)	DEW (Tol=1e-6)
1	187.9	186.3	187.9
2	27.7	27.5	27.7
3	5.8	5.8	5.8
4	5.8	5.7	5.8
5	59.0	58.8	59
6	159.3	160.9	159.3
7	21.2	21.0	21.2
8	3.4	3.3	3.4
9	9.2	9.1	9.2
10	9.5	9.0	9.5
11	2.4	2.5	2.4
12	3.2	2.2	3.2
13	1.3	0.7	1.3
14	10.3	10.9	10.3
15	5.8	5.8	5.8
16	20.5	19.9	20.5
17	19.3	18.9	19.3
18	10.4	10.6	10.4
19	33.3	33.4	33.3
20	6.0	5.7	6
21	17.6	17.3	17.6
22	56.4	55.0	56.4
23	12.8	13.0	12.8
24	10.3	10.1	10.3
25	11.6	11.6	11.6
26	14.4	13.1	14.4
27	10.8	26.1	10.7
28	11.6	11.6	11.6
29	23.0	35.9	23
30	8.9	-7.1	8.9
31	12.4	-3.0	12.4
32	15.1	11.4	15.1
33	3.5	-0.2	3.5
34	19.5	20.6	19.5
35	0.03	0.1	0.03
36	0.1	0.2	0.1
37	5.9	6.3	5.9
38	5.8	5.7	5.8
39	5.7	5.5	5.7

Pipe ID	EPANET	DEW (Tol = 1e-4)	DEW (Tol=1e-6)
40	5.8	5.6	5.8
41	5.8	5.4	5.8
42	17.5	17.8	17.5
43	17.3	16.9	17.3
44	6.0	9.0	6
45	35.6	38.5	35.6
46	63.0	61.0	63
47	26.6	27.3	26.6
48	15.0	15.7	15
50	22.5	22.6	22.5
51	9.2	9.0	9.2
52	9.6	10.1	9.6
53	2.4	2.6	2.4
54	3.4	3.2	3.4
55	18.0	17.9	18
56	2.1	2.2	2.1
57	10.1	9.9	10.1
58	1.5	1.7	1.5
59	5.8	5.8	5.8

2.9 Conclusions

The comparison of the solution methods offered valuable insight into how EPANET and DEW perform hydraulic calculations. The comparison of the simulation of the simple water distribution network in EPANET and DEW allowed for a preliminary assessment of the hydraulic simulating component in DEW. The following are the main conclusions drawn from this study:

1. Showing how the Todini method (gradient method) solved a network with the use of matrices provided a better understanding of how EPANET executes simulations. The flow predictions from all three solution methods were very close in value. This supports the notion that the bisection method used by DEW will converge on an acceptable solution if given enough time. The main

disadvantage of DEW's bisection method is the number of iterations required for convergence. On the other hand, the use of the Todini method allowed for a converged solution by the fifth iteration due to the fact that all of the nodal heads and pipe flows were determined in each iteration. Including the Hardy-Cross solution method allowed for the better understanding of DEW's approach due to their similarities. The DEW method attempts to solve each loop (cotree) individually and can inadvertently readjust a cotree that has satisfied the convergence criteria. This adjustment is illustrated in Figure 2.10. The plot shows that between the 14^{th} and 20^{th} iterations DEW fluctuated from what appeared to be a converged solution. This fluctuation is a result of DEW making an adjustment on one cotree that adversely affected the estimate through the other cotree. However, DEW appears to have corrected itself by the 25^{th} iteration.

2. The simulation of the simple looped network in Figure 2.11 in EPANET and DEW improved the understanding of DEW's hydraulic simulation capabilities. The results from this comparison revealed the sensitivity of DEW to set tolerance values. The DEW model may not converge on the best solution if a user has inputted an inappropriate tolerance value. This was demonstrated by how close the flow values from EPANET and DEW were when DEW's tolerance value was set to $1x10^{-6}$ from $1x10^{-4}$. The root mean square value for the difference between EPANET and DEW decreased from 4.1 to 0.028 gpm when the tolerance was changed to $1x10^{-6}$, which indicated that the flow values were much closer in value once the tolerance was decreased.

2.10 Future Work

Further research could be conducted in the comparison of EPANET and DEW. For instance, the solution methods that were used to solve the small network could be extended to a larger network. Using the solution methods to solve a larger network could offer further insight into the performance of the different methods. Performing an analysis using a larger network that consisted mainly of loops could reveal more advantages and disadvantages among the solution methods. For instance, the advantages from using the Todini method over the current DEW and Hardy-Cross methods could become more prevalent when the solution methods are used to solve a larger looped network.

The simple looped network that was simulated in EPANET and DEW offered a preliminary comparison of the two models. However, using a larger, more complex network could offer much more insight into the performance of the DEW model. Once the DEW model has reached the point in its development where complex hydraulic simulations occur without issue, the simulation of a large, complex network could be compared with the predicted values from EPANET. This comparison would provide valuable information that if necessary could be used to troubleshoot the hydraulic component of the DEW model.

During the simulation in DEW it became apparent that it was difficult to distinguish when crossing pipes with ends that had the same coordinates were not actually connected. This means that two pipes that appear to be connected may actually overlap each other (one pipe is deeper than the other). This issue can be addressed further to develop a way for DEW to identify whether pipes are connected or overlapping.

The use of pump and volume curves for pumps and tanks respectively will be added to the DEW model. The use of these curves will allow DEW to be used as a design model in addition to a real-time simulator connected to a SCADA system.

The solution approach used by DEW could be improved in several ways. The following are possible improvements to the hydraulic simulating component in the DEW model:

1. Improve Loop/Cotree Correction: Hardy-Cross Solution

   As previously discussed, the use of the Hardy-Cross method may be beneficial for determining the flow corrections applied to a network. This method could be used in lieu of the predefined correction value that stays constant throughout the solving process. However, a complication that could arise from the use of the Hardy-Cross method is the initial flow estimates through the pipes.

2. Improve Initial Flow Estimates: Minimum Spanning Tree

   A possible means to determine the initial flow estimates could be the use of a minimum spanning tree. A minimum spanning tree transforms a looped network into a branched network in which a parameter of the pipes (i.e. pipe resistance or pipe length) is at a minimum. The following example will elaborate on this method (Bhave, P.R. 2006):

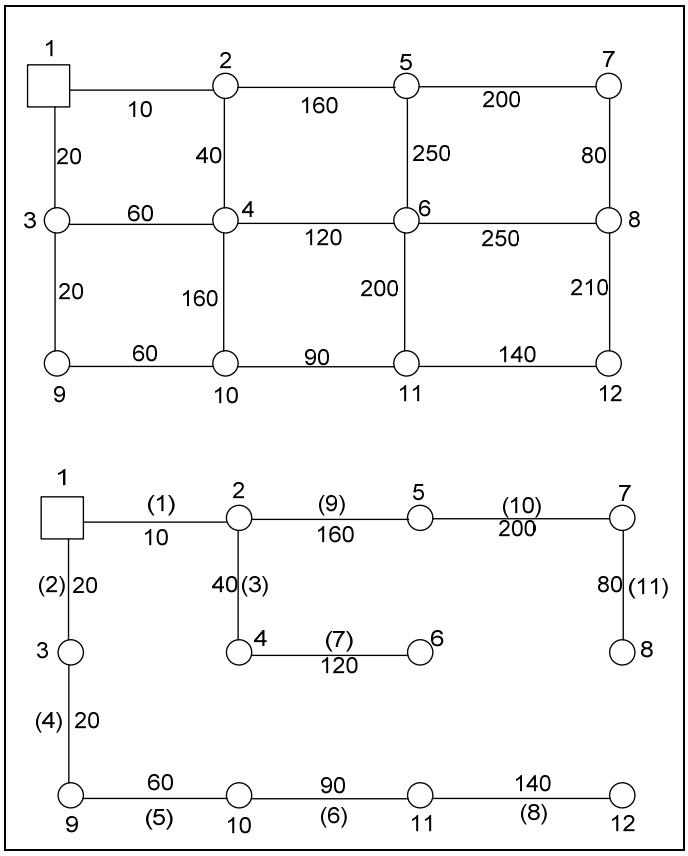

Figure 2.13: Minimum Spanning Tree Example

The pipe parameter considered in this example was pipe length. The first step in the example above was to consider the nodes connected to the source node (node 1). Thus, the first two nodes in consideration were nodes 2 and 3. The numbers in the parentheses are the order in which the pipes were added to the spanning tree. Since the pipe connecting node 1 to node 2 is shorter than the pipe connecting node 1 to node 3, it was the first pipe added to the spanning tree. Nodes 1 and 2 comprised the first partial spanning tree, and the nodes directly connected to this partial spanning tree were considered next (nodes 3, 4, and 5). Since the pipe connecting nodes 1 and 3 is shortest, it was the next pipe added to the spanning tree. This process continued until all of the nodes were accounted for and the maximum number of pipes was added without forming

a loop. With the minimum spanning tree constructed the initial flows could be determined using a simple branched network solution approach. All of the pipes that were not added to the spanning tree would contain an initial flow of zero. However, since the Hardy-Cross method cannot consider pipes with zero flow, a very small amount can initially flow through these pipes (i.e. $1x10^{-5}$ gpm). The incorporation of the use of a minimum spanning tree in the DEW model could be further explored.

3. Modified Solution: Bisection to Modified Todini Approach

   The current solution method for DEW will change. It is proposed that the radial portions of a system will be solved separately from the looped sections which will be solved using a matrix. The looped matrix solution is similar to the Todini method. However, instead of using a full matrix approach, DEW's method will use a matrix to determine the change applied to the flows in a loop similar to the upper part of the Todini matrix equation:

$$[A][dQ] = [-dE] \qquad \text{Eq. 2.6}$$

   The new flows will then be used to solve the pressure difference at the cotrees. This solution will continue until all of the pressure differences at the cotrees have satisfied the tolerance value.

The water distribution simulation capabilities of DEW will be advanced with the further exploration and development of the topics discussed above. A greater understanding of the DEW model and the implications that accompany a multidiscipline simulator will come from additional studies during the course of the model's development.

References

Bhave, P.R. and Gupta, R. (2006). “Hardy Cross method.” *Analysis of Water Distribution Networks,* Alpha Science Int’l Ltd., 187-188

Feinauer, L., Russell, K., and Broadwater, R. (2008). "Graph trace analysis and generic algorithms for interdependent reconfigurable system design and control." *Naval Engineers Journal,* 120.

Rossman, L.A. (2000) EPANET 2 Users Manuel. Water Supply and Water Resources Division *National Risk Management Research Laboratory.*

Todini, E. and Pilati, S. (1987). "A gradient algorithm for the analysis of pipe networks." *Computer Applications in Water Supply,* Research Studies Press Ltd., Taunton, UK., 1-20.

Appendix

Todini Solution:

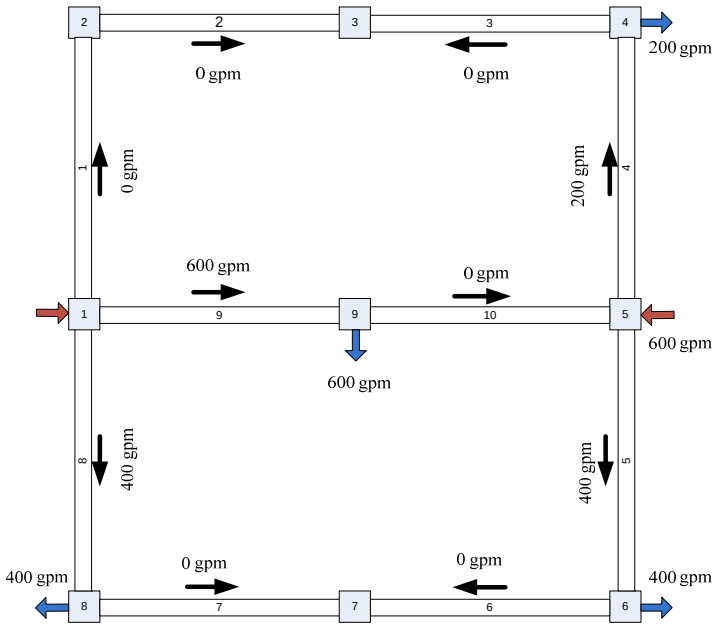

Figure A.1: Initial Flows and Directions for Todini Solution

Table A.1: Pipe Parameters

Link	Diam	Length
	in	ft
1	6	2000
2	6	1000
3	6	1000
4	6	2000
5	6	2000
6	6	1000
7	6	1000
8	6	2000
9	6	2000
10	6	2000

Table A.2: Network Parameters

C =	100	Assumed same for all pipes
n =	1.852	
H1 =	100 psi	
fixed	219.048 ft	

Iterations 1-4:

Iterations 5-8:

Iterations 9-12:

Hardy-Cross Solution:

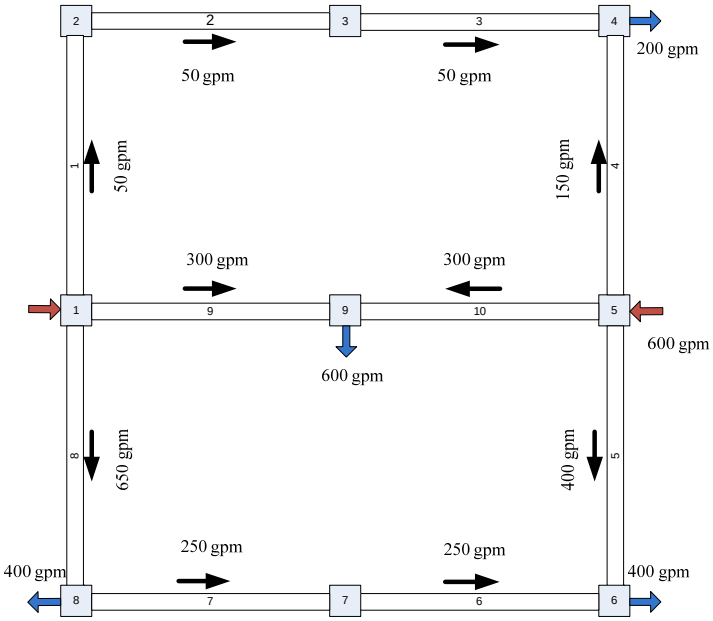

Figure A.2: Initial Flows and Directions for Hardy-Cross Solution

Iterations 1-3:

ITERATION 1						
Link	Diam	Length	Flow	hL	hL/Q	New Flow
	in	ft	gpm	ft	ft/gpm	gpm
1	6	2000	50	0.950607	0.019012	61.10
2	6	1000	50	0.475303	0.009506	61.10
3	6	1000	50	0.475303	0.009506	61.10
4	6	2000	-150	-7.27159	0.048477	-138.90
10	6	2000	300	26.25046	0.087502	311.10
9	6	2000	-300	-26.2505	0.087502	-288.90
			SUM	-5.37038	0.261505	
			DELTA Q	11.1008		
9	6	2000	288.9	24.47996	0.084735	433.39
10	6	2000	-311.1	-28.0777	0.090253	-166.61
5	6	2000	150	7.27159	0.048477	294.50
6	6	1000	-250	-9.36404	0.037456	-105.50
7	6	1000	-250	-9.36404	0.037456	-105.50
8	6	2000	-650	-109.907	0.169087	-505.50
			SUM	-124.961	0.467465	
			DELTA Q	144.4952		
ITERATION 2						
Link	Diam	Length	Flow	hL	hL/Q	New Flow
	in	ft	gpm	ft	ft/gpm	gpm
1	6	2000	61.10079	1.378057	0.022554	156.79
2	6	1000	61.10079	0.689028	0.011277	156.79
3	6	1000	61.10079	0.689028	0.011277	156.79
4	6	2000	-138.899	-6.3065	0.045403	-43.21
10	6	2000	166.6	8.832374	0.053014	262.30
9	6	2000	-433.4	-51.882	0.119711	-337.70
			SUM	-46.6	0.263235	
			DELTA Q	95.6906		
9	6	2000	337.7	32.68563	0.096788	381.61
10	6	2000	-262.3	-20.4697	0.07804	-218.39
5	6	2000	294.5	25.36537	0.086132	338.40
6	6	1000	-105.5	-1.89487	0.01796	-61.60
7	6	1000	-105.5	-1.89487	0.01796	-61.60
8	6	2000	-505.5	-68.9934	0.136484	-461.60
			SUM	-35.2018	0.433364	
			DELTA Q	43.9077		
ITERATION 3						
Link	Diam	Length	Flow	hL	hL/Q	New Flow
	in	ft	gpm	ft	ft/gpm	gpm
1	6	2000	156.7914	7.893058	0.050341	177.83
2	6	1000	156.7914	3.946529	0.025171	177.83
3	6	1000	156.7914	3.946529	0.025171	177.83
4	6	2000	-43.2086	-0.72541	0.016789	-22.17
10	6	2000	218.4	14.58015	0.066762	239.42
9	6	2000	-381.6	-40.9894	0.107411	-360.58
			SUM	-11.3485	0.291645	
			DELTA Q	21.0336		
9	6	2000	360.6	36.90377	0.102346	369.93
10	6	2000	-239.4	-17.287	0.072203	-230.07
5	6	2000	338.4	32.81106	0.096959	347.76
6	6	1000	-61.6	-0.69943	0.011355	-52.24
7	6	1000	-61.6	-0.69943	0.011355	-52.24
8	6	2000	-461.6	-58.3074	0.126317	-452.24
			SUM	-7.27847	0.420534	
			DELTA Q	9.3555		

Iterations 4-6:

ITERATION 4						
Link	Diam	Length	Flow	hL	hL/Q	New Flow
	in	ft	gpm	ft	ft/gpm	gpm
1	6	2000	177.825	9.965409	0.056041	183.16
2	6	1000	177.825	4.982705	0.02802	183.16
3	6	1000	177.825	4.982705	0.02802	183.16
4	6	2000	-22.175	-0.21089	0.00951	-16.84
10	6	2000	230.1	16.05689	0.069792	235.40
9	6	2000	-369.9	-38.6966	0.104604	-364.60
			SUM	-2.91981	0.295988	
			DELTA Q	5.3322		
9	6	2000	364.6	37.66998	0.103318	366.85
10	6	2000	-235.4	-16.7529	0.071168	-233.15
5	6	2000	347.8	34.51076	0.099238	350.01
6	6	1000	-52.2	-0.51552	0.009868	-49.99
7	6	1000	-52.2	-0.51552	0.009868	-49.99
8	6	2000	-452.2	-56.1377	0.124132	-449.99
			SUM	-1.74091	0.417592	
			DELTA Q	2.2535		
ITERATION 5						
Link	Diam	Length	Flow	hL	hL/Q	New Flow
	in	ft	gpm	ft	ft/gpm	gpm
1	6	2000	183.1572	10.52588	0.057469	184.47
2	6	1000	183.1572	5.262942	0.028735	184.47
3	6	1000	183.1572	5.262942	0.028735	184.47
4	6	2000	-16.8428	-0.12671	0.007523	-15.53
10	6	2000	233.1	16.4571	0.070587	234.46
9	6	2000	-366.9	-38.1023	0.103862	-365.54
			SUM	-0.72015	0.296911	
			DELTA Q	1.3111		
9	6	2000	365.5	37.8505	0.103546	366.09
10	6	2000	-234.5	-16.6289	0.070925	-233.91
5	6	2000	350.0	34.92606	0.099785	350.56
6	6	1000	-50.0	-0.47509	0.009504	-49.44
7	6	1000	-50.0	-0.47509	0.009504	-49.44
8	6	2000	-450.0	-55.6207	0.123605	-449.44
			SUM	-0.42327	0.41687	
			DELTA Q	0.5488		
ITERATION 6						
Link	Diam	Length	Flow	hL	hL/Q	New Flow
	in	ft	gpm	ft	ft/gpm	gpm
1	6	2000	184.4683	10.66585	0.057819	184.79
2	6	1000	184.4683	5.332925	0.02891	184.79
3	6	1000	184.4683	5.332925	0.02891	184.79
4	6	2000	-15.5317	-0.10906	0.007021	-15.21
10	6	2000	233.9	16.55688	0.070784	234.23
9	6	2000	-366.1	-37.9558	0.103678	-365.77
			SUM	-0.17629	0.297122	
			DELTA Q	0.3207		
9	6	2000	365.8	37.89426	0.103601	365.91
10	6	2000	-234.2	-16.5989	0.070867	-234.09
5	6	2000	350.6	35.02756	0.099919	350.69
6	6	1000	-49.4	-0.46548	0.009415	-49.31
7	6	1000	-49.4	-0.46548	0.009415	-49.31
8	6	2000	-449.4	-55.4952	0.123476	-449.31
			SUM	-0.10326	0.416693	
			DELTA Q	0.1340		

Iterations 7-9:

ITERATION 7						
Link	Diam	Length	Flow	hL	hL/Q	New Flow
	in	ft	gpm	ft	ft/gpm	gpm
1	6	2000	184.789	10.70022	0.057905	184.87
2	6	1000	184.789	5.350109	0.028953	184.87
3	6	1000	184.789	5.350109	0.028953	184.87
4	6	2000	-15.211	-0.10492	0.006898	-15.13
10	6	2000	234.1	16.58137	0.070832	234.17
9	6	2000	-365.9	-37.92	0.103633	-365.83
			SUM	-0.04308	0.297173	
			DELTA Q	0.0784		
9	6	2000	365.8	37.90493	0.103614	365.86
10	6	2000	-234.2	-16.5917	0.070852	-234.14
5	6	2000	350.7	35.05235	0.099951	350.73
6	6	1000	-49.3	-0.46315	0.009393	-49.27
7	6	1000	-49.3	-0.46315	0.009393	-49.27
8	6	2000	-449.3	-55.4645	0.123445	-449.27
			SUM	-0.02521	0.41665	
			DELTA Q	0.0327		
ITERATION 8						
Link	Diam	Length	Flow	hL	hL/Q	New Flow
	in	ft	gpm	ft	ft/gpm	gpm
1	6	2000	184.8674	10.70862	0.057926	184.89
2	6	1000	184.8674	5.354311	0.028963	184.89
3	6	1000	184.8674	5.354311	0.028963	184.89
4	6	2000	-15.1326	-0.10392	0.006867	-15.11
10	6	2000	234.1	16.58736	0.070844	234.16
9	6	2000	-365.9	-37.9112	0.103622	-365.84
			SUM	-0.01052	0.297185	
			DELTA Q	0.0191		
9	6	2000	365.8	37.90753	0.103618	365.85
10	6	2000	-234.2	-16.5899	0.070849	-234.15
5	6	2000	350.7	35.0584	0.099959	350.74
6	6	1000	-49.3	-0.46258	0.009388	-49.26
7	6	1000	-49.3	-0.46258	0.009388	-49.26
8	6	2000	-449.3	-55.4571	0.123437	-449.26
			SUM	-0.00616	0.416639	
			DELTA Q	0.0080		
ITERATION 9						
Link	Diam	Length	Flow	hL	hL/Q	New Flow
	in	ft	gpm	ft	ft/gpm	gpm
1	6	2000	184.8865	10.71068	0.057931	184.89
2	6	1000	184.8865	5.355338	0.028966	184.89
3	6	1000	184.8865	5.355338	0.028966	184.89
4	6	2000	-15.1135	-0.10368	0.00686	-15.11
10	6	2000	234.2	16.58882	0.070847	234.16
9	6	2000	-365.8	-37.9091	0.103619	-365.84
			SUM	-0.00257	0.297188	
			DELTA Q	0.0047		
9	6	2000	365.8	37.90817	0.103618	365.85
10	6	2000	-234.2	-16.5894	0.070848	-234.15
5	6	2000	350.7	35.05988	0.099961	350.74
6	6	1000	-49.3	-0.46244	0.009387	-49.26
7	6	1000	-49.3	-0.46244	0.009387	-49.26
8	6	2000	-449.3	-55.4552	0.123436	-449.26
			SUM	-0.0015	0.416636	
			DELTA Q	0.0020		

Iterations 10-12:

ITERATION 10						
Link	Diam	Length	Flow	hL	hL/Q	New Flow
	in	ft	gpm	ft	ft/gpm	gpm
1	6	2000	184.8912	10.71118	0.057932	184.89
2	6	1000	184.8912	5.355588	0.028966	184.89
3	6	1000	184.8912	5.355588	0.028966	184.89
4	6	2000	-15.1088	-0.10362	0.006858	-15.11
10	6	2000	234.2	16.58918	0.070847	234.16
9	6	2000	-365.8	-37.9085	0.103619	-365.84
			SUM	-0.00063	0.297189	
			DELTA Q	0.0011		
9	6	2000	365.8	37.90832	0.103619	365.85
10	6	2000	-234.2	-16.5893	0.070848	-234.15
5	6	2000	350.7	35.06024	0.099962	350.74
6	6	1000	-49.3	-0.4624	0.009387	-49.26
7	6	1000	-49.3	-0.4624	0.009387	-49.26
8	6	2000	-449.3	-55.4548	0.123435	-449.26
			SUM	-0.00037	0.416636	
			DELTA Q	0.000476		

ITERATION 11						
Link	Diam	Length	Flow	hL	hL/Q	New Flow
	in	ft	gpm	ft	ft/gpm	gpm
1	6	2000	184.8923	10.7113	0.057933	184.89
2	6	1000	184.8923	5.35565	0.028966	184.89
3	6	1000	184.8923	5.35565	0.028966	184.89
4	6	2000	-15.1077	-0.10361	0.006858	-15.11
10	6	2000	234.2	16.58927	0.070848	234.15
9	6	2000	-365.8	-37.9084	0.103619	-365.85
			SUM	-0.00015	0.297189	
			DELTA Q	0.000279		
9	6	2000	365.8	37.90836	0.103619	365.85
10	6	2000	-234.2	-16.5893	0.070848	-234.15
5	6	2000	350.7	35.06033	0.099962	350.74
6	6	1000	-49.3	-0.4624	0.009386	-49.26
7	6	1000	-49.3	-0.4624	0.009386	-49.26
8	6	2000	-449.3	-55.4547	0.123435	-449.26
			SUM	-9E-05	0.416636	
			DELTA Q	0.000116		

ITERATION 12						
Link	Diam	Length	Flow	hL	hL/Q	New Flow
	in	ft	gpm	ft	ft/gpm	gpm
1	6	2000	184.8926	10.71133	0.057933	184.89
2	6	1000	184.8926	5.355665	0.028966	184.89
3	6	1000	184.8926	5.355665	0.028966	184.89
4	6	2000	-15.1074	-0.1036	0.006858	-15.11
10	6	2000	234.2	16.58929	0.070848	234.15
9	6	2000	-365.8	-37.9084	0.103619	-365.85
			SUM	-3.7E-05	0.297189	
			DELTA Q	6.8E-05		
9	6	2000	365.8	37.90837	0.103619	365.85
10	6	2000	-234.2	-16.5893	0.070848	-234.15
5	6	2000	350.7	35.06035	0.099962	350.74
6	6	1000	-49.3	-0.46239	0.009386	-49.26
7	6	1000	-49.3	-0.46239	0.009386	-49.26
8	6	2000	-449.3	-55.4547	0.123435	-449.26
			SUM	-2.2E-05	0.416636	
			DELTA Q	2.84E-05		

Iterations 13-15:

ITERATION 13						
Link	Diam	Length	Flow	hL	hL/Q	New Flow
	in	ft	gpm	ft	ft/gpm	gpm
1	6	2000	184.8927	10.71134	0.057933	184.89
2	6	1000	184.8927	5.355668	0.028966	184.89
3	6	1000	184.8927	5.355668	0.028966	184.89
4	6	2000	-15.1073	-0.1036	0.006858	-15.11
10	6	2000	234.2	16.5893	0.070848	234.15
9	6	2000	-365.8	-37.9084	0.103619	-365.85
			SUM	-9.1E-06	0.297189	
			DELTA Q	1.66E-05		
9	6	2000	365.8	37.90837	0.103619	365.85
10	6	2000	-234.2	-16.5893	0.070848	-234.15
5	6	2000	350.7	35.06036	0.099962	350.74
6	6	1000	-49.3	-0.46239	0.009386	-49.26
7	6	1000	-49.3	-0.46239	0.009386	-49.26
8	6	2000	-449.3	-55.4547	0.123435	-449.26
			SUM	-5.3E-06	0.416636	
			DELTA Q	6.93E-06		
ITERATION 14						
Link	Diam	Length	Flow	hL	hL/Q	New Flow
	in	ft	gpm	ft	ft/gpm	gpm
1	6	2000	184.8927	10.71134	0.057933	184.89
2	6	1000	184.8927	5.355669	0.028966	184.89
3	6	1000	184.8927	5.355669	0.028966	184.89
4	6	2000	-15.1073	-0.1036	0.006858	-15.11
10	6	2000	234.2	16.5893	0.070848	234.15
9	6	2000	-365.8	-37.9084	0.103619	-365.85
			SUM	-2.2E-06	0.297189	
			DELTA Q	4.06E-06		
9	6	2000	365.8	37.90837	0.103619	365.85
10	6	2000	-234.2	-16.5893	0.070848	-234.15
5	6	2000	350.7	35.06036	0.099962	350.74
6	6	1000	-49.3	-0.46239	0.009386	-49.26
7	6	1000	-49.3	-0.46239	0.009386	-49.26
8	6	2000	-449.3	-55.4547	0.123435	-449.26
			SUM	-1.3E-06	0.416636	
			DELTA Q	1.69E-06		
ITERATION 15						
Link	Diam	Length	Flow	hL	hL/Q	New Flow
	in	ft	gpm	ft	ft/gpm	gpm
1	6	2000	184.8927	10.71134	0.057933	184.89
2	6	1000	184.8927	5.355669	0.028966	184.89
3	6	1000	184.8927	5.355669	0.028966	184.89
4	6	2000	-15.1073	-0.1036	0.006858	-15.11
10	6	2000	234.2	16.5893	0.070848	234.15
9	6	2000	-365.8	-37.9084	0.103619	-365.85
			SUM	-5.4E-07	0.297189	
			DELTA Q	9.91E-07		
9	6	2000	365.8	37.90837	0.103619	365.85
10	6	2000	-234.2	-16.5893	0.070848	-234.15
5	6	2000	350.7	35.06036	0.099962	350.74
6	6	1000	-49.3	-0.46239	0.009386	-49.26
7	6	1000	-49.3	-0.46239	0.009386	-49.26
8	6	2000	-449.3	-55.4546	0.123435	-449.26
			SUM	-3.2E-07	0.416636	
			DELTA Q	4.14E-07		

DEW Solution:

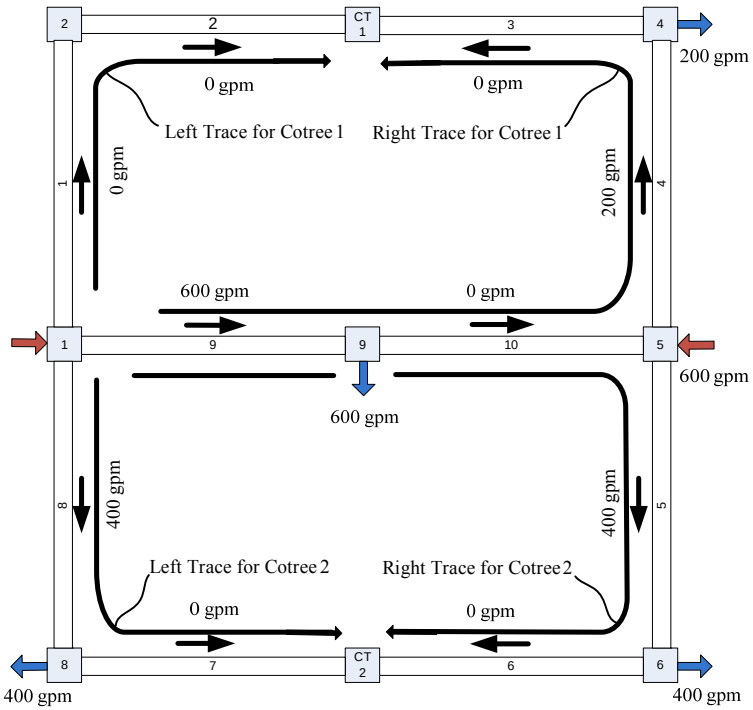

** CT 1and CT 2 are the locations of cotree 1 and cotree 2 respectively*

Figure A.3: Initial Flows and Directions for DEW Solution

Iterations 1-3:

Iteration 1				
Pipe ID	Flow (gpm)	Length (ft)	hf (ft)	psi
1	0	2000	0.00	0.00
2	0	1000	0.00	0.00
3	0	1000	0.00	0.00
4	200	2000	12.39	5.37
5	400	2000	44.72	19.38
6	0	1000	0.00	0.00
7	0	1000	0.00	0.00
8	400	2000	44.72	19.38
9	600	2000	94.76	41.06
10	0	2000	0.00	0.00

cotree 1 Δp = (100-(0+0))-(100-(41.06+0+5.37+0)) = 46.43 psi

cotree 2 Δp = (100-(19.38+0))-(100-(41.06+0+19.38+0)) = 41.06 psi

Iteration 2				
Pipe ID	Flow (gpm)	Length (ft)	hf (ft)	psi
1	71.9	2000	1.86	0.81
2	71.9	1000	0.93	0.40
3	71.9	1000	0.93	0.40
4	128.1	2000	5.43	2.35
5	400	2000	44.72	19.38
6	0	1000	0.00	0.00
7	0	1000	0.00	0.00
8	400	2000	44.72	19.38
9	528.1	2000	74.81	32.42
10	71.9	2000	1.86	0.81

cotree 1 Δp = (100-(0.81+0.40))-(100-(32.42-0.81+2.35-0.40)) = 32.35 psi

cotree 2 Δp = (100-(19.38+0))-(100-(32.42-0.81+19.38+0)) = 31.61 psi

Iteration 3				
Pipe ID	Flow (gpm)	Length (ft)	hf (ft)	psi
1	143.8	2000	6.72	2.91
2	143.8	1000	3.36	1.46
3	143.8	1000	3.36	1.46
4	56.2	2000	1.18	0.51
5	400	2000	44.72	19.38
6	0	1000	0.00	0.00
7	0	1000	0.00	0.00
8	400	2000	44.72	19.38
9	456.2	2000	57.05	24.72
10	143.8	2000	6.72	2.91

cotree 1 Δp = (100-(2.91+1.46))-(100-(24.72-2.91+0.51-1.46)) = 16.49 psi

cotree 2 Δp = (100-(19.38+0))-(100-(24.72-2.91+19.38+0)) = 21.81 psi

Iterations 4-6:

Iteration 4				
Pipe ID	Flow (gpm)	Length (ft)	hf (ft)	psi
1	143.8	2000	6.72	2.91
2	143.8	1000	3.36	1.46
3	143.8	1000	3.36	1.46
4	56.2	2000	1.18	0.51
5	328.1	2000	30.99	13.43
6	71.9	1000	0.93	0.40
7	71.9	1000	0.93	0.40
8	471.9	2000	60.74	26.32
9	384.3	2000	41.53	17.99
10	215.7	2000	14.25	6.17

cotree 1 Δp = (100-(2.91+1.46))-(100-(17.99-6.17+0.51-1.46)) = 6.50 psi

cotree 2 Δp = (100-(26.32+0.40))-(100-(17.99-6.17+13.43-0.40)) = -1.88psi

Iteration 5				
Pipe ID	Flow (gpm)	Length (ft)	hf (ft)	psi
1	215.7	2000	14.25	6.17
2	215.7	1000	7.12	3.09
3	215.7	1000	7.12	3.09
4	15.7	2000	0.11	0.05
5	328.1	2000	30.99	13.43
6	71.9	1000	0.93	0.40
7	71.9	1000	0.93	0.40
8	471.9	2000	60.74	26.32
9	312.5	2000	28.31	12.27
10	287.5	2000	24.26	10.51

cotree 1 Δp = (100-(6.17+3.09))-(100-(12.27-10.51-0.05-3.09)) = -10.64 psi

cotree 2 Δp = (100-(26.32+0.40))-(100-(12.27-10.51+13.43-0.40)) = -11.95 psi

Iteration 6				
Pipe ID	Flow (gpm)	Length (ft)	hf (ft)	Pressure (psi)
1	215.7	2000	14.25	6.17
2	215.7	1000	7.12	3.09
3	215.7	1000	7.12	3.09
4	15.7	2000	0.11	0.05
5	400	2000	44.72	19.38
6	0	1000	0.00	0.00
7	0	1000	0.00	0.00
8	400	2000	44.72	19.38
9	384.3	2000	41.53	17.99
10	215.7	2000	14.25	6.17

cotree 1 Δp = (100-(6.17+3.09))-(100-(17.99-6.17-0.05-3.09)) = -0.578 psi

cotree 2 Δp = (100-(19.38+0))-(100-(17.99-6.17+19.38-0)) =11.819 psi

Iterations 7-8:

Iteration 7				
Pipe ID	Flow (gpm)	Length (ft)	hf (ft)	Pressure (psi)
1	179.7	2000	10.16	4.40
2	179.7	1000	5.08	2.20
3	179.7	1000	5.08	2.20
4	20.3	2000	0.18	0.08
5	328.1	2000	30.99	13.43
6	71.9	1000	0.93	0.40
7	71.9	1000	0.93	0.40
8	471.9	2000	60.74	26.32
9	348.4	2000	34.63	15.01
10	251.6	2000	18.95	8.21

cotree 1 Δp = (100-(4.40+2.20))-(100-(15.01-8.21+0.08-2.20)) = -1.935 psi

cotree 2 Δp = (100-(26.32+0.40))-(100-(15.01-8.21+13.43-0.40)) =-6.907psi

Iteration 8				
Pipe ID	Flow (gpm)	Length (ft)	hf (ft)	Pressure (psi)
1	179.7	2000	10.16	4.40
2	179.7	1000	5.08	2.20
3	179.7	1000	5.08	2.20
4	20.3	2000	0.18	0.08
5	364.1	2000	37.57	16.28
6	35.9	1000	0.26	0.11
7	35.9	1000	0.26	0.11
8	435.9	2000	52.44	22.72
9	384.3	2000	41.53	17.99
10	215.7	2000	14.25	6.17

cotree 1 Δp = (100-(6.17+3.09))-(100-(17.99-6.17-0.05-3.09)) = -0.578 psi

cotree 2 Δp = (100-(19.38+0))-(100-(17.99-6.17+19.38-0)) =11.819 psi